A Hitch-Hiker's Guide to VLA Observing Strategies

Alan H. Bridle
National Radio Astronomy Observatory
Charlottesville, Virginia, U.S.A.

Text last updated: 11 July 1996
HTML version available at:
http://www.cv.nrao.edu/vla/hhg2vla/hhg2vla.html

Contents

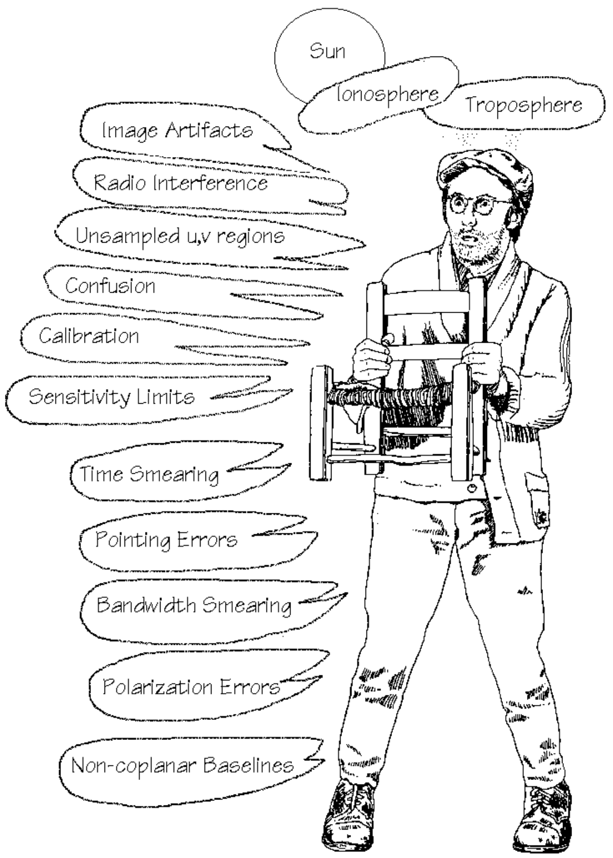

Figure 1: "The NRAO Welcomes Your VLA Observing Proposal"

1 Introduction

Many of the other lectures in this course emphasize problems that corrupt the images made by synthesis radio telescopes under real conditions. By this point, you may feel that you need a mixture of good luck and magic to get useful results from such telescopes. If the images can be degraded in so many ways, how does anyone get useful science from the VLA (Figure 1)?

My goal is to explain how to avoid *many* of the worst imaging pathologies when planning a synthesis observation. There is at least one orderly approach to minimizing the problems you will encounter. So, in the spirit of another *Hitch-Hiker's Guide* (Adams 1979)—"**DON'T PANIC!**".

The approach described here can be used when planning observations with *any* synthesis radio telescope.

Sections 3, 4 and 5 of this lecture work through a suggested decision tree (Section 2) for planning continuum observations.

Section 6 deals with the problem of unwanted sources in the field, and what to do about them.

Section 7 outlines a similar decision tree for spectral line work. The strategies disussed in these Sections should help you to meet your scientific goals by minimizing the worst image defects—those that would affect even perfectly-calibrated data.

Section 8 reviews points that you should consider when planning how to calibrate your data. Section 9 describes what (little) can be done to modify your observing strategy once the data are actually being taken.

To separate ideas which may apply to other synthesis telescopes from details that are quirks of the VLA, I have herded the latter into an Appendix (Section 10). This Appendix also describes some resources, available from the NRAO, which may help you when planning VLA observing proposals.

Lecture 20 tackles similar strategic questions in the context of VLBI, especially the VLBA.

2 The Continuum Observer's Decision Tree

Figure 2 shows the decision tree that I suggest for continuum observers.

Section 3 starts work at the top left of this tree, asking how much resolution $\theta_{\rm HPBW}$ is wanted, and at what frequency ν_0.

Sections 4 and 5 work down the tree to estimate the total observing time $t_{\rm int}$ that would be needed to meet your initial requirements. Whether to proceed "as is" depends on whether this first observing-time estimate, and the associated data volume, seem reasonable.

3 Resolution, Baseline Range and Observing Frequency

3.1 Angular resolution: how much is enough?

The first step is to determine the *range* of angular resolution $\theta_{\rm HPBW}$ that is appropriate for the project. You should think about both the minimum and maximum values of $\theta_{\rm HPBW}$.

The lowest resolution (*maximum* value of the synthesized beam width $\theta_{\rm HPBW}$) will be set by your need to separate, or to resolve, astrophysically important features of the region being imaged. Realize however that you can have *too much* resolution if your project depends on imaging *extended* emission. There is no point observing extended emission using such a small beamwidth $\theta_{\rm HPBW}$ that crucial features are close to, or below, the r.m.s. noise ΔI_m on the final images. You must therefore estimate the *apparent brightness* (flux density per synthesized beam area) that you expect important extended features to have at the resolution you will use for your final images. You can then determine the highest resolution (*minimum* $\theta_{\rm HPBW}$) that is appropriate for your project by estimating the total integration time $t_{\rm int}$ needed to reach the required brightness sensitivity. As omitting this aspect of the project design can render the final images useless, it is worth restating the principles.

Recall from Lecture 4 that a *point* source with flux density S Jy images with an apparent brightness of S Jy per synthesized beam area regardless of the area $\Omega_{\rm s}$ of the synthesized beam. It follows that, for any synthesis array of identical antennas and receivers, all baselines are equally sensitive to a given point source (apart from the effects of confusion and phase stability). In contrast, the apparent brightness of an *extended* emission region in a synthesized image depends on the region's detailed structure, on how well the visibility function $V(u, v)$ is sampled by the observations, and on the weighting and tapering functions D_k and T_k applied to the data when imaging (Lecture 7). When deciding on an observing strategy, it usually suffices to assume that:

- an extended region with uniform true brightness I Jy per square arcsec will be imaged with an apparent brightness $\approx I\Omega_{\rm s}$ Jy per synthesized beam area $\Omega_{\rm s}$, and
- the *final* synthesized beam will be a Gaussian `CLEAN` beam, so that its area $\Omega_{\rm s}$ will be $\approx 1.13\theta_1\theta_2$ square arcsec, where θ_1 and θ_2 are the major and minor half-power widths of the Gaussian in arcsec.

If the r.m.s. noise on the image is ΔI_m Jy per synthesized beam, the signal-to-noise ratio of such extended emission on the image will be $\sim I\Omega_{\rm s}/\Delta I_m$, which increases as the synthesized beam area $\Omega_{\rm s}$. You must ensure that you do not observe at such small values of $\Omega_{\rm s}$ that interesting extended

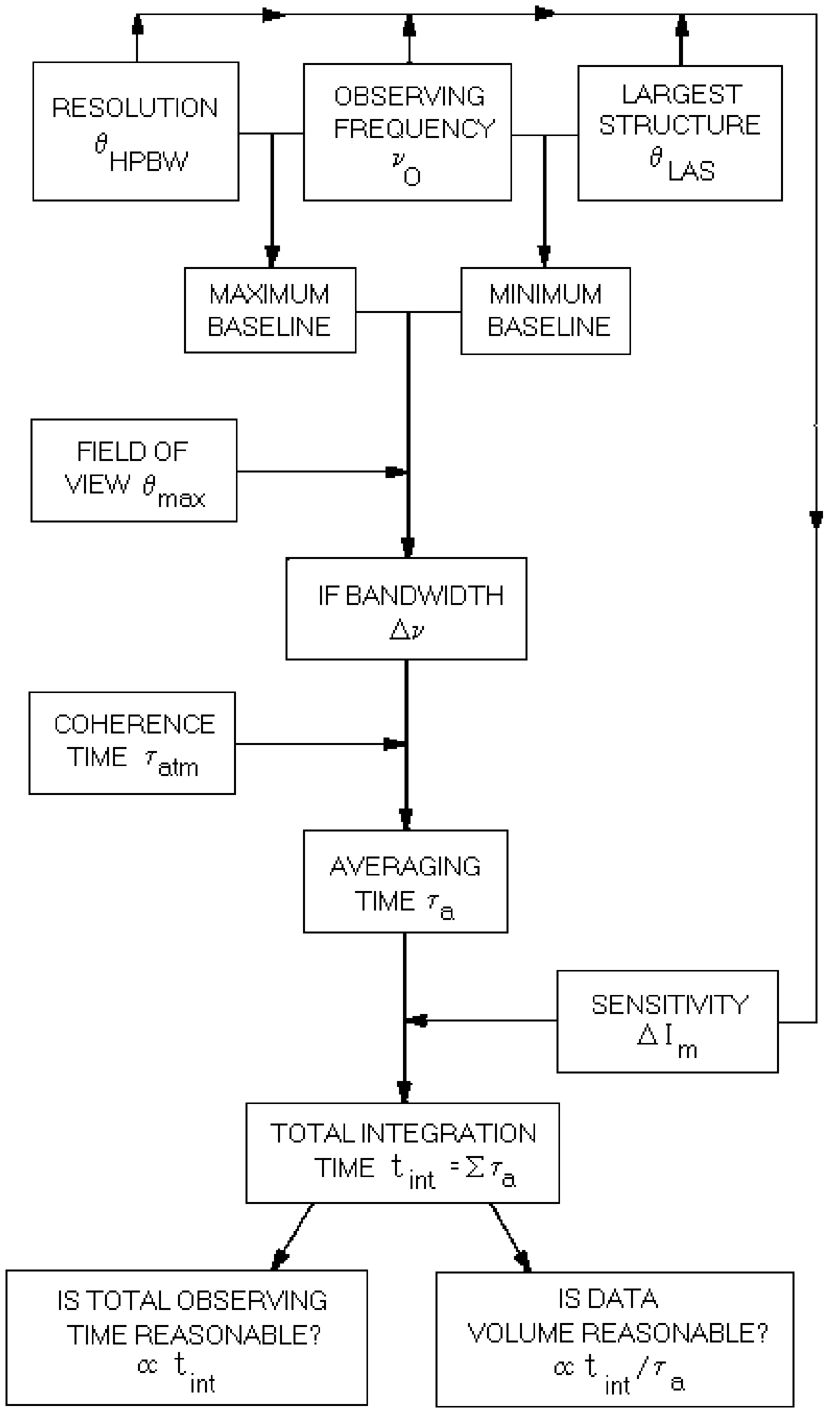

Figure 2: Factors Affecting Continuum Observing Strategy—A Suggested Decision Tree.

structure is undetectable, given the total integration time $t_{\rm int}$ available and your choice of the IF bandwidth $\Delta\nu$ (see Sections 4 and 5below).

There are circumstances however when enhanced resolution helps you to detect interesting features—for example, when searching for pointlike "hot spots" or linear "jets" in more diffuse emission such as large scale "lobes". While the flux density per synthesized beam of two-dimensional emission is roughly proportional to the beam *area* $\Omega_{\rm s}$, that of linear emission is proportional to the beam *width* $\theta_{\rm HPBW}$, and that of a point source is *independent* of beam size. These dependencies allow compact structure that is embedded in, or confused with, more extended emission to be recognized most easily on high-resolution images.

Note that it is also important to avoid unnecessarily high resolution (long baselines) in detection experiments. Although the *theoretical* sensitivity to a point source is independent of the size of the array (apart from the effects of confusion), the phase fluctuations produced by atmospheric irregularities will be greater on longer baselines (Lectures 5 and 6). It is therefore more difficult to reach the theoretical sensitivity by integrating coherently between calibrations when using long-baseline arrays. This is especially true at high frequencies, where the phase stability depends critically on conditions in the troposphere over the array. The severity of ionospheric or tropospheric phase fluctuations varies from site to site, and at any one site with the "weather" from hour to hour, from day to day, and from season to season. It is generally true however that observations longer than about an hour with $\theta_{\rm HPBW} < 1$" are often corrupted by atmospheric phase fluctuations and that observations with $\theta_{\rm HPBW} < 0\overset{\prime\prime}{.}1$ *always* are. The most powerful tool for dealing with these corruptions is self-calibration (Lecture 9). This technique is rarely applicable to detection experiments, however—unless they are unusually successful, so that all detected sources are strong!

3.2 Largest Structure

The next step in planning your observations involves thinking about $\theta_{\rm LAS}$, the largest angular scale of structure that you must sample well to produce a useful final image. $\theta_{\rm LAS}$ will be the angular diameter of the most extended structure that you must image accurately. This will usually be the diameter of the most extended component of your target that is of astrophysical interest.

Do not confuse $\theta_{\rm LAS}$ with $\theta_{\rm max}$, the required field of view, which is discussed below. When observing a target $10''$ in extent in the presence of a point confusing source $1'$ away, you would set $\theta_{\rm LAS} = 10''$, not $\theta_{\rm LAS} = 1'$.

$\theta_{\rm LAS}$ determines the *shortest* baseline length that you need in your data for the images to be useful. The visibility of a circular Gaussian source with FWHM $\theta_{\rm LAS}$ falls to half of its peak amplitude at a normalized baseline length of $91{,}000/\theta_{\rm LAS}$ wavelengths, if $\theta_{\rm LAS}$ is in arc seconds. You will not be able to image a two-dimensional structure of size $\theta_{\rm LAS}$ well unless *projected* baselines at least this short are present in the data. Depending on the density of tracks in the inner u-v plane, and on the sensitivity per baseline, more conservative criteria may be needed—halving the above estimate gives a baseline on which the visibility falls to about 85% of its peak. Note also that the detailed array geometry, target declination and hour-angle range determine how baselines are foreshortened by projection. The most reliable approach is therefore to look at u-v plots for your expected antenna layout, declination, and hour-angle range to ensure that your planned short-baseline coverage meets the requirements imposed by $\theta_{\rm LAS}$. (This can be done for any antenna array using the program `UVSIM` in the NRAO's Astronomical Image Processing System.)

The factors affecting the choice of resolution cannot be estimated reliably in advance if the source structure is poorly known. If you are not sure what your source may look like, its is safer to guess on the side of low resolution when designing an initial observation. A "diagnostic" low resolution image may tell you the source's total angular extent, and warn you about surrounding emission. This information will let you optimize the parameters for a more time-consuming high resolution study. It is also easier to justify reobserving a detected emission region at high resolution than to justify reobserving at low resolution what previously appeared to be empty sky!

3.3 Choice of frequency at given resolution

Continuum observers will choose the observing frequency *at a given resolution* by balancing astronomical criteria against instrumental performance. A high frequency may be necessary for polarimetry because Faraday effects decrease with increasing frequency (degrees of linear polarization are generally higher at higher frequencies and electric vectors lie closer to their intrinsic position angles). Polarimetric data are also less corrupted by the Earth's ionosphere at high frequencies. Studies of Faraday effects (e.g., depolarization) in continuum sources may demand low observing frequencies, however. The spectral index of the continuum also influences the choice of frequency—optically thick thermal emission may be easier to detect at high frequencies whereas transparent synchrotron sources will be easier to detect at low frequencies.

If a continuum project has frequency agility, the choice of ν_0 also involves the receiver sensitivity and antenna performance as a function of frequency. High frequency observations are often limited by worsening receiver noise performance, antenna efficiency and pointing accuracy (as a fraction of the primary beam size) with increasing frequency. Low frequency observations are limited by interference at many radio observatories.

3.3.1 Interference

The detailed choice of observing frequency, especially below 2 GHz, is often constrained by known sources of radio frequency interference (RFI). For example, U.S. frequency allocations in the L Band around 20 cm include aeronautical radio navigation (including global satellite networks), meteorological aids, and fixed and mobile use. Many of the possible external interfering signals are time variable, so freedom from external interference can never be guaranteed at L Band outside the protected radio astronomy bands. The protected band from 1400 to 1427 MHz is undesirable for some continuum observations, however, because galactic neutral hydrogen emission can increase the system temperature significantly in this band.

External interfering signals are partially rejected by interferometers (e.g., Thompson 1982) because only the component of the signals that (a) varies at the sidereal fringe rate, and (b) correlates with the correct delay, will affect the output. In practice, this combination makes low frequencies and short-baseline synthesis arrays more sensitive to RFI than high frequencies (where radio frequency band allocations are less congested) and long-baseline arrays.

Data averaging reduces the response to interfering signals by the factor $\mathrm{sinc}(\nu_f \tau_c)$ where ν_f is the natural fringe frequency and τ_c is the time over which the data are averaged when computing the visibility in each u-v cell before Fourier transforming. As $\nu_f = \omega_e u \cos\delta$, where ω_e is the angular velocity of the Earth's rotation and δ is the declination, fringe rate rejection is least for observations near the celestial poles and for baselines near the v-axis, where fringe frequencies are near zero. In a given RFI environment, long-baseline arrays collect more data at large values of u than do short-baseline arrays, so long-baseline arrays are less affected by RFI (unless the RFI is strong enough to degrade the noise performance of the individual receivers). Short-baseline arrays may also suffer more from locally-generated RFI or from "crosstalk" (correlations between signals radiated by the electronics of one antenna directly into the feed or the electronics of another).

Delay rejection is a more complex function of the azimuth of the baseline and the position of the interfering source, as described in detail by Thompson (1982). Its effects cannot be stated as concisely as those of fringe rate rejection and are not a simple function of location in the u-v plane. Delay rejection is not usually significant for narrow-band interfering signals.

RFI may always be edited from the data after they are taken (with particular attention to data falling near the v-axis), but careful choice of observing frequency can minimize both the effort necessary for editing and the consequent loss of data.

3.3.2 Imaging at more than one frequency

When studying spectral index, Faraday rotation or depolarization properties of extended sources, you should attempt to minimize uncertainties arising from differing resolutions at the different frequencies. It is important to try to "scale" the distributions of baseline lengths in *wavelengths* that are used for the different observations. Ideally, you would scale the detailed distribution of antenna spacings but it is often difficult to scale more than the inner and outer baseline limits and the tapering and weighting functions (especially when observing with fixed arrays, as in VLBI). You should also make the hour-angle ranges of the observations at different frequencies as similar as possible.

Note that although using such "scaled arrays" *optimizes your chances* of measuring frequency-dependent properties of a source accurately, it cannot *guarantee* success. Even scaled arrays may have significantly different relative sensitivities to different scales of structure if the structure changes radically with frequency, e.g., if there are large spectral index gradients in either the total or polarized emission. You must also be careful when interpreting the final images if the databases at different frequencies are differently affected by missing antennas or by bad data. In many cases, the reliability of inter-frequency comparisons depends on how well the deconvolution algorithm (Lecture 9) interpolates unsampled parts of the u-v plane, even when scaled arrays have been used.

Observing at several adjacent, but not necessarily contiguous, frequency bands can improve the u-v coverage, and so help you to reconstruct complex structures with high fidelity, by "bandwidth synthesis". For this application, observing frequencies should be spaced to minimize the sizes of residual "holes" in the u-v coverage. For example, if the largest "holes" $\Delta u, \Delta v$ in the coverage at one frequency are about 10% of the corresponding radii $\sqrt{u^2+v^2}$, data from two observing frequencies separated by 5% might be combined.

4 Field of View Restrictions

Once you have settled on the resolution θ_{HPBW}, baseline range and observing frequency ν_0 for your program, the next decision (see Fig. 2 again) involves IF bandwidth $\Delta\nu$ and averaging time τ_{a}. These must be consistent with the field of view requirements of your program. You must therefore consider the radius θ_{max} (from the center of the field of view) over which you require the data to be minimally distorted by chromatic aberration and time-average smearing as discussed in Lectures 3 and 10 (and in Bridle & Schwab 1989).

4.1 Continuum: IF bandwidth

An unsuitable choice of the IF bandwidth $\Delta\nu$ may lead (a) to irrecoverable distortion of the image by chromatic aberration if the bandwidth is too great or (b) to unacceptably low sensitivity if it is too small.

As discussed in detail by Bridle & Schwab (1989), images made with finite bandwidth are degraded away from the delay tracking center in a way that can be described as a radial smearing by a position-dependent distortion function. The width of the distortion function grows with distance from the delay tracking center. The effect can be thought of as a reduction in amplitude, and a simultaneous broadening, of the apparent point source response. Bridle & Schwab derive expressions for the amplitude reduction $R_{\Delta\nu} = I/I_0$ (where I is the observed amplitude and I_0 is the amplitude in the small-bandwidth limit) for three combinations of bandpass shapes and u-v tapering. All three are functions of the simple dimensionless parameter $\beta = (\Delta\nu/\nu) \times (\theta/\theta_{\mathrm{HPBW}})$, i.e. of the fractional bandwidth times the angle from the delay tracking center measured in synthesized half-power beamwidths:

1. $R_{\Delta\nu} = \frac{2}{3.79\beta}\mathrm{Si}\frac{3.79\beta}{2}$ for a square bandpass and u-v coverage with no tapering, Si being the standard sine integral,

2. $R_{\Delta\nu} = \frac{\sqrt{\pi}}{\gamma\beta}\mathrm{erf}\frac{\gamma\beta}{2}$ ($\gamma \equiv 2\sqrt{\ln 2} = 1.665$), for a square bandpass with circular Gaussian u-v tapering, erf being the error function, and

3. $R_{\Delta\nu} = \frac{1}{\sqrt{1+\beta^2}}$ for a Gaussian bandpass with circular Gaussian u-v tapering.

The first step in choosing the IF bandwidth for continuum work is to ask over what field radius $\theta_{\rm max}$ (arcsec) you want to limit chromatic aberration to a given reduction of amplitude $R_{\Delta\nu}$ of the point source response. Then find the corresponding maximum value $\beta_{\rm max}$ of the normalized parameter β from whichever expression for $R_{\Delta\nu}$ best approximates your instrument. The maximum allowable IF bandwidth $\Delta\nu_{\rm max}$ (MHz) consistent with these constraints is then given by

$$\Delta\nu_{\rm max} = \frac{\beta_{\rm max}\nu_0\theta_{\rm HPBW}}{\theta_{\rm max}}, \tag{1}$$

where ν_0 is your observing frequency in MHz and $\theta_{\rm HPBW}$ is the half-power beamwidth in arcsec at which you expect to make your images. Unless you are prepared to relax your smearing/attenuation criterion slightly, select the closest allowed bandwidth that is *narrower* than $\Delta\nu_{\rm max}$. If you are prepared to relax it, choose the closest *wider* bandwidth.

Your choice of $\theta_{\rm max}$ may be determined by the need to image an extended structure with minimal distortion, or by the need to include a strong confusing source in the minimally-distorted field of view. The latter need arises because you may wish to subtract or deconvolve a confusing source's sidelobes from the interesting region. The value of $\theta_{\rm max}$ will always be greater than, or about equal to, the value of $\theta_{\rm LAS}$ used earlier when selecting the range of baselines. In general, choose the delay and pointing center to minimize the required $\theta_{\rm max}$ for your observations. When using a wide field to include a confusing source, consider displacing the delay center away from the target towards the confusing source. This will avoid the use of unnecessarily narrow bandwidths (and thus of unnecessarily low sensitivity). If the field is *dominated* by a strong point source (more than ten times brighter than other structure), *this* source should be placed near the delay center and pointing center when high dynamic range is required. This strategy will minimize the total distortion of the image resulting from bandwidth, pointing, averaging time and computational effects (such as u-v truncation) involving the strong source (for more details, see Clark 1981).

For point source detection experiments the above criteria will normally select the widest available bandwidth, unless the search position is exceptionally inaccurate or the field is known to be highly confused. Chromatic aberration affects observing strategy less critically at higher frequencies for several practical reasons—fractional bandwidths ($\Delta\nu/\nu_0$) are often smaller; the usable field of view is limited by the primary HPBW of the antennas for the narrower fractional bandwidths; receiving systems are noisier and antennas are less efficient (so sensitivity, not distortion, limits image quality).

When deciding on the value of $\theta_{\rm max}$ that is appropriate for an image of an extended source, consider the detectability of the extended emission *at the resolution you will be using for your images* (see Sections 3 and 5). There is no point ensuring that extended structure is not smeared radially by the bandwidth effect if low signal-to-noise on the same structure introduces uncertainties larger than the bandwidth distortions. As the signal-to-noise on extended emission itself depends on the choice of IF bandwidth, this calculation may need to be iterated until a suitable compromise is reached.

4.2 Visibility averaging time

It is important to choose the "on-line" averaging time $\tau_{\rm a}$, i.e., the averaging applied to the data before they are written to an initial storage medium, carefully. The data will be averaged relative to a particular phase tracking center and this on-line averaging cannot be undone. Any excess averaging done off-line, after the data have been archived, can be undone later, though it is obviously inefficient to do this.

The effects of finite averaging time $\tau_{\rm a}$ were outlined in Lectures 3 and 10, and are also discussed in detail by Bridle & Schwab (1989), whose results I simply quote here. As $\tau_{\rm a}$ is increased, phase winding of a point source at radius θ from the phase center both smears and attenuates the synthesized response to such a source. The effect is worst on a given baseline when Earth rotation moves the source perpendicular to the fringes associated with that baseline, but is zero when the feature moves parallel to the fringes. The magnitude of the effect therefore depends on baseline orientation, hour-angle and declination. For an array observing a point source near the north celestial pole, the *average* reduction in amplitude $\overline{\langle R_\tau \rangle}$ can be estimated in terms of the angular distance θ from the phase tracking center as:

$$\overline{\langle R_\tau \rangle} = \frac{I}{I_0} = 1 - \eta \left(\frac{\theta}{\theta_{\rm HPBW}} \right)^2 \tau_{\rm a}^2 \, , \tag{2}$$

where

- $\eta = 1.05 \times 10^{-9}$ for uniform square u-v coverage,
- $\eta = 1.08 \times 10^{-9}$ for uniform circular u-v coverage and
- $\eta = 1.22 \times 10^{-9}$ for circular, Gaussian tapered, u-v coverage, and
- $\tau_{\rm a}$ is in seconds.

The choice of $\tau_{\rm a}$ balances several issues. First, you must decide what amplitude reduction R_τ due to time-average smearing will be acceptable at $\theta = \theta_{\rm max}$. Then estimate the corresponding $\tau_{\rm a}$ from Equation 2 using appropriate values of η and $\theta_{\rm HPBW}$. If sensitivity or hardware considerations force you to choose an IF bandwidth that is wider than the $\Delta\nu_{\rm max}$ given by Equation 1, estimate $\tau_{\rm a}$ so that the effects of time-average smearing at $\theta_{\rm max}$ are slightly less than those of chromatic aberration. (See Section 10.4 for a VLA-based example.)

Ideally, you would observe with $\tau_{\rm a}$ set to the value estimated from Equation 2 unless this exceeds the expected coherence time $\tau_{\rm atm}$ for the atmospheric phase fluctuations on the longest baselines, or unless it is too long to let you edit the data satisfactorily. In either of those cases, you would observe with a shorter $\tau_{\rm a}$. You may later average the edited, calibrated data to the value estimated from Equation 2, to minimize the data volume and the image processing time.

5 Total Integration Time

Once you have determined the IF bandwidth $\Delta\nu$ from the field of view criteria, the next step in the continuum decision tree (Fig. 2) the continuum decision tree is to estimate the total on-source integration time $t_{\rm int}$ required for given sensitivity on your final image. Here you will use the expression for the r.m.s. noise ΔI_m on an image made with an N-antenna array:

$$\Delta I_m = F_w \Delta S \Bigg/ \sqrt{\frac{nN(N-1)}{2} t_{\rm int} \Delta\nu} \, , \tag{3}$$

where n is the number of independent IFs contributed to the image per antenna ($n = 2$ for images of Stokes I from two orthogonal polarization states at one sky frequency, or for images of $P = \sqrt{Q^2 + U^2}$ at one sky frequency), $t_{\rm int}$ is in seconds, and $\Delta\nu$ is in MHz. In the numerator, $F_w = 1.0$ for natural weighting and is > 1 for other weightings (the value depending on the gridding and on the baseline distribution—see Lecture 8 for VLA-specific details). ΔS is the single-interferometer sensitivity per second per MHz of IF bandwidth.

The sensitivity goal will be determined by (a) the significance level you need for a detection to achieve your astronomical goals, and (b) whether the interesting emission is extended (see Section 3.1above). If you are doing polarimetry, calculate the sensitivity from the expected *polarized* intensity, not total intensity.

You have now reached a critical decision. You have an estimate of the total on-source integration time $t_{\rm int}$ needed for the project as you would initially prefer to do it. Adding some overhead for calibration (typically 10% to 20%, but see Section 8 for details), you now have an idea of how much observing time you would need.

If this first estimate of the total observing time is much longer than the time that the source is above the elevation limits of the telescope each day, then consider carefully whether your choices of frequency and baseline range were optimal. You may wish to re-enter the decision tree with different starting parameters before taking the proposal further.

If your $t_{\rm int}$ is about as long as the source is visible each day, then your project may be well suited to making a full-synthesis image. You could then adjust the observations to fit into a single pass of the source across the sky.

If your $t_{\rm int}$ is much less than the time that the source is visible each day, your observing strategy will be determined by the need for dynamic range (i.e. for good u-v coverage) and by whether you can merge observations of several such sources into one program. If you need high dynamic range, or you want to image an extended structure with $t_{\rm int}$ less than needed for a full synthesis, you should still sample the u-v plane as uniformly as possible. This can usually be done satisfactorily by distributing the observing over several short (e.g., $\sim$ 10-minute) scans spaced equally through the available hour-angle range. Note however that the dynamic range achieved in a given observation also depends on atmospheric and ionospheric conditions, on the elevation angle range, and on your calibration strategy (Section 8below), as well as on the u-v coverage.

Two-dimensional arrays with many antennas may have good enough instantaneous u-v coverage to make a “snapshot” mode attractive for observations of strong, compact sources when the total integration time required is small. Section 10.7 discusses the advantages and disadvantages of snapshot mode at the VLA.

6 Confusing Sources

Confusion may have two effects on the interpretation of a synthesis image:

- the r.m.s. fluctuation level on the image may be degraded by sidelobes or by aliasing of confusing sources, and
- an extraneous radio source may be mistaken for the target in a detection experiment, or considered part of the structure of an extended feature.

The best way to handle confusion is to learn about it in the context of your particular target field. Before you observe, consult published radio surveys, or low resolution images of the field around your target, for possible confusion. If you know you will be observing near a bright confusing source, you may consider either of two strategies for reducing its effects on your final images.

If the confusion is relatively nearby, plan to look at it—to make wide-field images containing both the target and the confusing source. Then subtract or deconvolve the confusing source and its sidelobes from the interesting region. The ungridded subtraction technique (Lecture 9—coded in the NRAO `AIPS` package as the programs `MX` and `IMAGR`) helps this strategy, as only the parts of the wide field that contain significant emission need to be computed and deconcolved (`CLEAN`ed). This approach can work well if the confusing source is only one or two times as far from the target as the radius of the field of view that you would otherwise have imaged. If the confusing source is strong, consider displacing the delay tracking center away from the target toward the confusion, to minimize distortions of the response to the confusing source by chromatic aberration and other effects.

If the confusion is relatively distant, try *not* to look at it—choose your IF bandwidth and the delay, phase and pointing centers to minimize the response to the confusing source. Note that because the point source attenuation produced by chromatic aberration and time averaging increases with baseline length $\sqrt{u^2+v^2}$, these effects do not filter confusing sources from the short-baseline data as effectively as they do from long-baseline data. If a distant confusing source still dominates the data after attenuation by the primary beam, it may therefore produce wide-angle "ripple" in the final image. In such cases, the pointing center should be chosen to minimize the response to the confusion rather than to maximize the response to the target.

A difficult case arises when the response to the confusing source is strong even after adopting this stratagem. Variable pointing errors and (for altitude–azimuth antenna mounts) the rotation of the primary sidelobe pattern of the antennas on the sky may then make the confusing source appear to vary throughout the observation. It is hard to make images with high dynamic range in these circumstances (see also Lecture 10). It is worth recognizing this difficulty before observing, if only because you might be able to select an alternative target that is equally interesting.

If a confusing source lies in the target field itself, no advance precautions are necessary, as the confusing source and its sidelobe pattern can be deconvolved from the image as part of normal data reduction. Note however that it is important to *look* for confusion *after* taking the data, e.g., by making a heavily-tapered low-resolution image covering as much sky as possible around your target. It is particularly important to do this before proceeding with computer-intensive processing such as deconvolution, or self-calibration at full resolution. Making low-resolution images to search for confusing sources early in your image processing may (a) improve the models used for self-calibration, (b) reveal unexpected large-scale structure around your target (and so help to define `CLEAN` deconvolution windows) and (c) lead to unexpected discoveries.

In detection experiments, confusion may make the interpretation of a positive detection questionable if a source is detected near, but not at, the target position. Source counts (e.g., Section 10.9) should be used to estimate the probability that the detected source lies in the image by chance.

7 The Spectroscopist's Decision Tree

The constraints to be balanced when designing a spectroscopic experiment differ slightly from those that face continuum observers, though some decisions are in common between the two styles of observing. Figure 3 shows a decision tree for spectral line observing.

7.1 Observing frequency

Many spectroscopic experiments have little (or no) choice of observing frequency. The line frequency is set by the chemical species and transition relevant to the astronomical problem. The observing frequency is then determined by correcting the line frequency for the systemic radial velocity and for the various motions of the Earth (see Lecture 11). For the experiment to be viable, the corrected frequency must, of course, lie within the tuning range of the receivers and feeds.

If the chemical species has many radio-frequency transitions (e.g., recombination lines), instrumental performance and astronomical criteria may again be combined when picking the observing frequency. For such projects, the instrumental criteria are similar to those for the continuum: receiver sensitivity, antenna efficiency, pointing accuracy. The astronomical criteria may include whether different transitions will be in emission, or absorption, or both.

The last factor to be considered is radio frequency interference (RFI). Some spectroscopic observations, especially those at frequencies below 2 GHz and those of objects whose red shifts move the observing frequency out of a protected band, are simply not possible because of RFI.

7.2 Spectroscopy: IF bandwidth

Two different IF bandwidths enter into the observing strategy for spectroscopy.

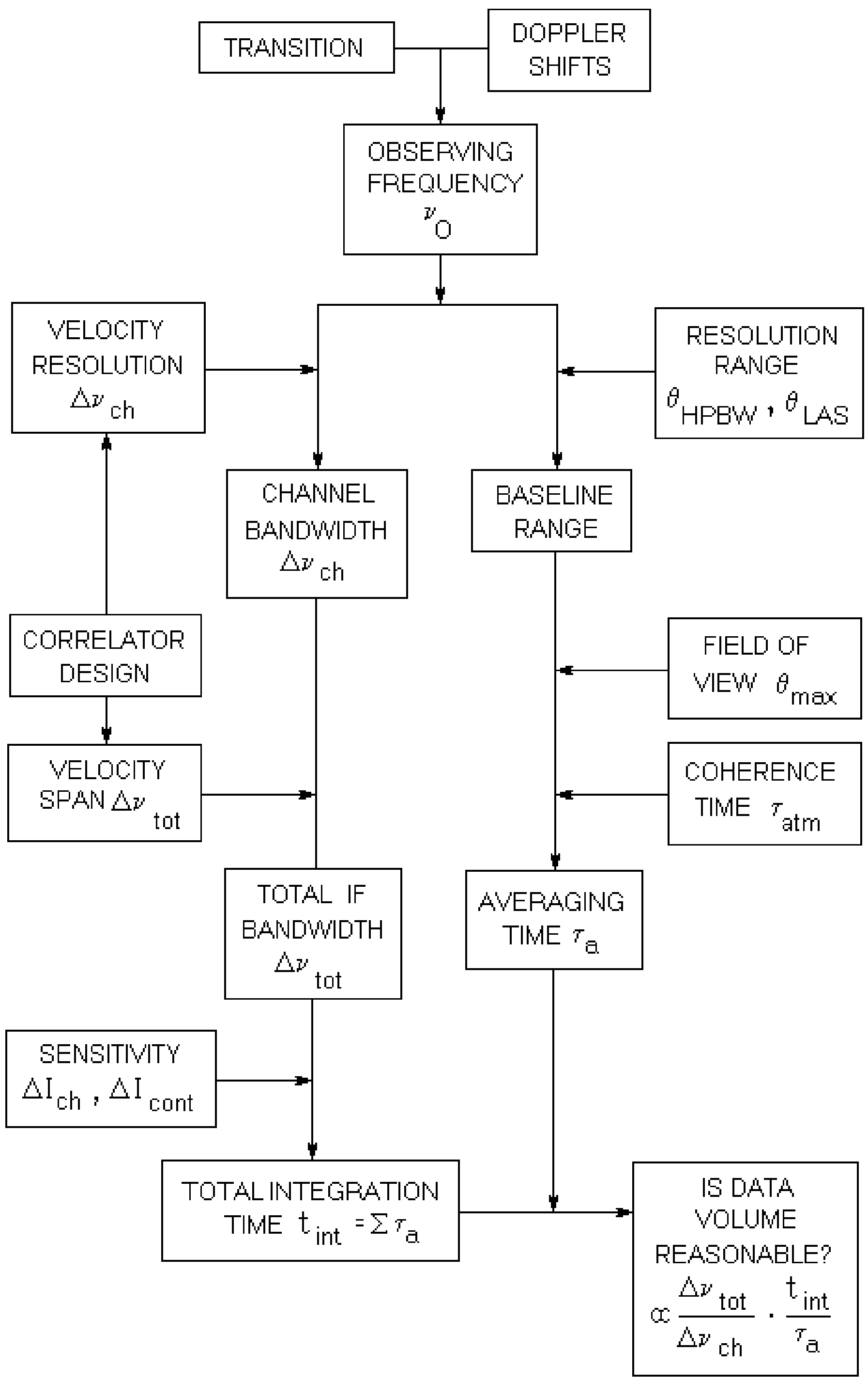

Figure 3: Factors Affecting Spectral Line Observing Strategy—A Suggested Decision Tree.

1. The *total* IF bandwidth $\Delta\nu_{\rm tot}$ that is spanned by all the line channels. $\Delta\nu_{\rm tot}$ determines the *range* of velocities included by the experiment, which should span not only the interesting parts of the line profile, but also an adequate number of line-free channels (allowing for any band-edge effects in autocorrelation spectrometers).

2. The individual *channel* bandwidth $\Delta\nu_{\rm ch}$. This sets the velocity *resolution* of the experiment. It also determines the chromatic aberration effects for the individual channel images.

As indicated in Figure 3, the choices of $\Delta\nu_{\rm tot}$ and $\Delta\nu_{\rm ch}$ are usually tightly coupled by the design of the spectral line correlator, and velocity resolution and velocity span must often be traded against one another.

The need for velocity resolution usually drives the *channel* bandwidth to a small enough value that individual channel images are negligibly smeared by chromatic aberration. This does not mean, however, that spectroscopists can ignore chromatic aberration in synthesis imaging. The *synthesized beam* pattern is different for every channel image when the channels are gridded separately with their correct frequencies. Any data reduction schemes that do not separately deconvolve the synthesized beam from each of the individual channel images may therefore "rediscover" effects related to the frequency dependence of the beam. As Lecture 12 describes, such separate deconvolution of all the channels is not always a good strategy. If you estimate the continuum distribution by summing the "dirty" images over a range of line-free channels, or if you difference two "dirty" line channel images, the variation of the synthesized beam with frequency may become apparent. If you try to avoid this effect for some channels by artificially assigning them the same frequency (to make the "dirty beam" the same for all images), you will restore the chromatic aberration corresponding to the widest channel separation $\Delta\nu_{tot}$ used in such processing.

7.3 Averaging time

Ideally, the averaging time $\tau_{\rm a}$ for spectroscopy will be determined by considering (a) the distortion produced by time-average smearing (Equation 2), and (b) the atmospheric coherence time $\tau_{\rm atm}$. Because narrow-band channel images are relatively free from chromatic aberration, it rarely makes sense to choose $\tau_{\rm a}$ for high-resolution spectroscopy by matching time-average smearing to chromatic aberration, as in some continuum experiments.

In practice, however, observations with narrow channel bandwidths may also require long *total* integration times $t_{\rm int}$ to reach sufficient signal-to-noise in the individual channel images. This interacts with the choice of $\tau_{\rm a}$, because a long averaging time may be needed simply to restrain the number of independently recorded visibilities. If $\tau_{\rm a}$ is limited by the data volume, Equation 2 should be used to check the distortion at the edge of the interesting field. If a $\tau_{\rm a}$ that keeps the data volume manageable also produces significant distortion, you may have to balance using (a) long averaging times $\tau_{\rm a}$ (image distortion), (b) wider channel bandwidths $\Delta\nu_{\rm ch}$ (poorer velocity resolution), (c) fewer channels $\Delta\nu_{\rm tot}/\Delta\nu_{\rm ch}$ (poorer velocity span), or (d) fewer antennas N (poorer image quality) to restrain the data volume ($\propto N(N-1) \times (t_{\rm int}/\tau_{\rm a}) \times (\Delta\nu_{\rm tot}/\Delta\nu_{\rm ch})$).

7.4 Sensitivity and total integration time

Spectroscopists may need to consider separately two different sensitivities—the sensitivity to spectral features in the individual line channels and the accuracy with which the continuum can be estimated from the line-free channels. The need for individual channel sensitivity normally dominates, however. The calculation uses Equation 3, with $\Delta\nu_{\rm ch}$ replacing $\Delta\nu$. It may also be appropriate to express the sensitivity in terms of brightness temperature by converting from mJy per beam area to temperature units assuming a Gaussian beam of area $\Omega_s = 1.13\theta^2_{\rm HPBW}$.

Use of narrow channel bandwidths $\Delta\nu_{\rm ch}$ often implies that sensitivity, rather than *u*-*v* coverage, considerations determine $t_{\rm int}$ for high-resolution synthesis spectroscopy, so that observations > 12 hours long may be needed. Spectroscopic observations may also need long integrations on the calibration sources to achieve enough sensitivity.

7.5 Time of day

Because spectroscopic experiments often use compact arrays and narrow bandwidths, they are more vulnerable than continuum observations to the effects of the Sun passing through the sidelobes of the array. Both short baseline lengths and narrow channel bandwidths reduce the spectroscopists' immunity from far-out sidelobe responses—this is one way in which continuum observers are helped by bandwidth smearing! The problems are especially severe at low observing frequencies at times of enhanced solar activity. Below 2 GHz, many spectroscopic experiments can be done only at night if the Sun is active.

8 Calibration Strategy

The basic issues to be decided by the observer are:

- what system-wide parameters will be known satisfactorily from special purpose calibrations done independently of the observing, and
- what time-dependent calibration parameters will be monitored, and how often, during the observing itself.

The first decision will vary from observatory to observatory and from project to project. It must be approached by reviewing all the calibration steps described in Lectures 5 through 7, and asking how well each calibration parameter will be known in advance relative to the needs of the project. I concentrate here on the second issue, which itself has two main parts—how often to monitor the instrument and the atmosphere by observing reference sources, or "calibrators", and how close the calibrators should be to the target(s). Your strategy will depend on whether you attempt to calibrate only the instrumental fluctuations, or these fluctuations plus the apparent amplitude and phase variations introduced by the ionosphere and troposphere (again, see Lectures 5 and 6 for details). Any calibration that monitors atmospheric fluctuations will, of course, calibrate instrumental fluctuations also.

8.1 Instrumental calibration

The instrumental calibration should:

- detect grossly malfunctioning antennas so that faults can be corrected while the observations are in progress, and
- monitor the amplitude and phase stability of the instrument rapidly enough that any changes can be corrected by interpolation throughout the run.

In a well-designed array, most instrumental fluctuations (apart from phase jumps) are slow, so that observations of an unresolved strong calibrator every few hours or more will monitor the instrument adequately. Bear in mind however that if the instrumental calibration detects a discontinuity such as a phase jump, you may have to discard all the data between consecutive calibration observations for the antenna-IF in which the jump occurred (unless the source being imaged is strong enough that the precise time of the jump can be located in the source data—in which case you can probably self-calibrate it anyway).

Calibrators for purely instrumental monitoring should be chosen primarily for their strength rather than for closeness to the target(s).

8.2 Atmospheric calibration

It is more important, and much more difficult, to calibrate amplitude and phase fluctuations that result from changes in the propagation properties along the atmospheric path to the target. Unfortunately, *no calibration based on observations of a phase reference source that is not in the same isoplanatic patch as the target can be guaranteed to improve the data quality.* This does not mean that attempts to calibrate atmospheric fluctuations using distant reference sources are a waste of time, but you must recognize that such "external" calibration may or may not be successful.

8.2.1 External calibration

If the target and calibrator are separated by an angle greater than that subtended by the atmospheric cells responsible for the amplitude and phase variations, the fluctuations seen in the calibrator data may not correlate with those in the target data. Corrections interpolated from the calibrator observations into the rest of the data under these circumstances may *worsen* the atmospheric amplitude and phase noise on the target by a factor of $\approx \sqrt{2}$. At the other extreme, if the target and calibrator are typically within the *same* isoplanatic patch, the fluctuations observed in the calibrator will faithfully track those occurring in the target. Amplitude and phase corrections interpolated into the target data from the calibrator data in time series may then greatly improve the quality of the final image. The basic problem is that the scale size of the isoplanatic patch will vary from day to day and even from hour to hour (as a function of the "weather" and of the elevation of your target above the horizon). It is therefore difficult to judge how reliable amplitude and phase referencing from a distant calibrator may be before the observations begin.

If you cannot, or do not wish to, rely on self-calibration to remove atmospheric effects from your data, you should choose external calibrator(s) as close as possible to the target(s), ideally within a degree or so of them. You must then hope that the amplitude and phase stability found in the calibrator data meet the needs of your experiment, and that the scale of the isoplanatic patch is typically greater than the calibrator–target separation.

If the within-scan *and scan-to-scan* amplitude or phase fluctuations on a calibrator a degree or two from your target are small (less than 10% or 20°), it is unlikely that much larger fluctuations are occurring on your target. Correcting the rest of the data using long-term averages of the calibrator phases is then likely to improve matters.

If you see large, rapid fluctuations on the calibrator, you are in trouble, which may or may not be mitigated by correcting the rest of the data by local (point-to-point) interpolation in the fluctuations. Because such interpolation may indeed make matters worse, you might then try making images (a) after long-term averaging, and (b) after local interpolation, of phase corrections from the calibrators. You can then judge empirically which gives better final images—using the final dynamic range, r.m.s. noise level, and/ or any prior knowledge about the source to make your judgment.

Deleting data from some or all baselines during periods of unusually bad phase stability will usually improve the quality of images made by external calibration. Imaging with less data but with good amplitude and phase stability can give better results than imaging with much poorly-calibrated data—if the synthesized beam is closer to the theoretical "dirty" beam, deconvolution algorithms work better, increasing the dynamic range of the images. Note that tapering the u-v data down-weights the visibilities from the longer baselines where phases are less stable. Be ready to sacrifice resolution in favor of forming the theoretical beam more closely when the phases are unstable, if your astronomical goals can be met at lower resolution.

Observers doing detection experiments are usually forced to use external calibration. Fortunately, they do not usually require such high dynamic range (and such good phase stability) as observers imaging bright emission complexes. The loss of point source response produced by poor phase stability in a detection experiment can be estimated by calibrating with a long (e.g., > 2 hour) interpolation of the gains, then imaging the calibrators and comparing their apparent flux densities in these images with their assumed values.

8.2.2 Self-calibration

The most reliable method for removing atmospheric fluctuations from the data is self-calibration, *if the target is strong enough.* Self-calibration should be used if the signal-to-noise on the target is high enough to determine the gains in the typical coherence time $\tau_{\rm atm}$ of the atmospheric phase screen, using baselines involving all antennas. For an array of N elements, the r.m.s. noise in the determination of an individual antenna phase gain by self-calibration on a point source of flux density S_{sc} Jy will be

$$\phi_{\rm rms} \approx \frac{65 \Delta S}{S_{sc}\sqrt{(N-2)\Delta\nu\tau_{\rm sc}}} \text{ degrees}, \tag{4}$$

where ΔS is the sensitivity in Jy per second per MHz of bandwidth, and $\tau_{\rm sc}$ is the averaging time used for the gain solutions. Unless $\phi_{\rm rms} \ll 60^\circ$ when $\tau_{\rm sc} = \tau_{\rm atm}$, self-calibration will not improve the data.

There are several reasons why external calibration is useful even if you know you will be able to self-calibrate your final images.

- External calibrators will provide flux-density and position scales for self-calibrated images (on which this information will otherwise generally be lost).
- Observations of the time scale of the phase fluctuations on a phase calibrator near your target can also be used to estimate the coherence time $\tau_{\rm atm}$ of the atmosphere during your observations. This will enable you to select a suitable averaging time $\tau_{\rm sc}$ for the self-calibration: it should be $\leq \tau_{\rm atm}$.
- External calibration may also tell you that some parts of your data were obtained under more stable atmospheric conditions than others; the "good" parts may yield a better initial model of your target that helps self-calibration of the whole data set to converge quickly.

Fortunately, the class of source for which images of high dynamic range are most important is also the class for which self-calibration is most likely to work well—namely, those with weak extended structures around bright small-diameter components. There is however a range of flux densities and structural complexities over which self-calibration cannot be guaranteed to work in typical atmospheric coherence times $\tau_{\rm atm}$, and for which external calibration therefore remains essential.

8.3 Position calibration

The phase referencing that is done during external calibration refers the absolute position scale of the images to the mean position scale defined by the adopted positions of the external phase calibrators, if the antenna co-ordinates are well determined. No further positional calibration is required for routine (non-astrometric) synthesis imaging. Note however that *self-calibration* fundamentally has no absolute phase reference and therefore produces images whose position scale is whatever was specified in the input model.

8.4 Flux density calibration

The flux density scale is usually set by observing an unresolved reference source whose flux density is believed to be stable and whose intensity has previously been measured on an absolute scale. As there are few such sources that remain unresolved to long-baseline arrays, it is rarely possible to use a primary flux density calibrator also as the primary phase calibrator. Good phase calibrators are strong and unresolved, so are likely to vary with time. The flux densities of phase calibrators must usually be determined at the time of the observations by measuring their amplitude ratios to standard flux density calibrators, often using only a short-baseline subset of all the antennas in the array. Note that self-calibration has no absolute amplitude scale and therefore produces images whose flux density scale is whatever was specified in the input model.

8.5 Polarization calibration

The quantities to be calibrated are the individual antenna cross-polarization terms and the position angle scale (including any time-variable ionospheric Faraday rotation). The design of this calibration depends on whether the antennas are on equatorial or altitude–azimuth mounts, and on the feed polarizations. The VLA case is described in Section 10.10.3.

8.6 Bandpass calibration

Spectroscopists must also calibrate the instrumental bandpass, often for both amplitude and phase. The amplitude calibration may sometimes be estimated by dividing the cross-correlation spectra by the geometric mean of the autocorrelation spectra of the relevant antennas. This approach is unsuitable however if there are lines (or interfering signals) in the passband that are strong enough to show up in the single-antenna spectra. It is inadequate if the phase variation across the band is significant relative to other uncertainties, for example those imposed by the signal-to-noise ratio.

The most complete approach to bandpass calibration is to observe a strong line-free continuum source to find the bandpass characteristics (amplitude and phase) of each antenna-receiver combination. In a well-engineered system, these characteristics will be only slow functions of time, so the calibration need not be repeated often. Notice however that the total time needed for the bandpass calibration is set by the sensitivity required to measure the gain *in each channel* as accurately as needed for the required *spectral* dynamic range. Projects that require high spectral dynamic range may therefore have to invest a large fraction of the total observing time in bandpass calibration. See Lecture 12 for details of bandpass calibration strategy.

9 Stormy Weather—Dynamic Scheduling

For some observing programs, it may be possible to adjust the observing strategy to take account of the weather during the observing run. But, to quote Barry Clark from the early days of operating the VLA under New Mexico's usually-sunny skies: "you can't tell the phase stability by looking out of the window". You must *observe* to find out how stable the phases are. It is difficult to guess phase stability in advance (except to say that it is likely to be bad because a storm front is passing, for example). But it is also difficult to predict it at the time of observing just by "looking out of the window". Clear blue skies offer a much better chance of stable phases than lowering clouds, thunderstorms or snow. But they do not guarantee freedom from upper-air turbulence and winds that may also produce unstable phases!

If your program has frequency agility and you are actually at the telescope, it is a good idea to monitor the phase of a strong calibrator for a few minutes on a long baseline as you start observing. Fluctuations of order a radian on a time scale of minutes are unmitigated bad news. The only possible strategy is to move the observations to lower frequencies if this makes astronomical sense. The converse is not true, however. Short-term (minute-by-minute) phase stability to within a few degrees does not guarantee that the observations will be of good quality for synthesis. Synthesis imaging requires stability over the time scale of your calibration cycle (unless you are going to self-calibrate). You should therefore pay attention to the phase changes between *adjacent* scans of your calibrator, as well as to that within the scans, to assess whether you have the stability needed for synthesis. If the longer-term stability is marginal, i.e., of order $30°$ to $40°$ between calibrations, you might consider using a faster calibration cycle.

The weather is the one area of synthesis observing where you truly do need a little luck, especially if you cannot self-calibrate your data!

10 Appendix: Considerations Specific to the VLA

To avoid obscuring general principles elsewhere, I have collected VLA-specific details into this Appendix. Users of other synthesis radio telescopes may find this Appendix helpful as a "worked example" of points discussed in the rest of the lecture.

10.1 Choosing a VLA Configuration

10.1.1 Standard configurations

An image made from untapered uniformly-weighted ≥ 4 hour tracks in a standard VLA configuration at declinations above $-15°$, where foreshortening of the array is relatively unimportant, has a synthesized beam whose half-power beamwidth is given approximately by

$$\theta_{\rm HPBW} = 1\overset{''}{.}3 \times \frac{1.5}{\nu_0} \times 3.3^{n-1}\,, \tag{5}$$

where ν_0 is the observing frequency in GHz and $n = 1, 2, 3,$ or 4 for the **A**, **B**, **C**, or **D** configuration, respectively. The exact beamwidth depends on declination, and on details of the u-v coverage. But this estimate will do for planning purposes.

It is crucial to choose a suitable combination of ν_0 and n when planning VLA observations. For example, suppose you want to study a smooth two-dimensional emission region $30''$ across whose peak apparent brightness $I\Omega_{\rm s}$ would be 1 mJy per `CLEAN` beam area on an untapered 20 cm image in the **B** configuration (resolution $\approx 4''$). It could be detected at the 10σ level in about 10 min of integration at 50 MHz bandwidth in the **B** configuration (using the sensitivity data given in Table 5 and natural weighting). This is an easy experiment!

But now suppose you try to image the same region using the **A** configuration, keeping everything else—observing frequency, tapering, u-v weighting, bandwidth—the same. The region will have a peak apparent brightness of only $\sim$0.1 mJy per beam area (the synthesized HPBW will now be $\approx 1\overset{''}{.}3$). A 10σ detection would therefore require about 14 hours of on-source integration! This shows why it is *extremely* important not to use a wider VLA configuration (i.e., smaller beam area $\Omega_{\rm s}$) than is strictly necessary, when studying *extended* emission.

The choice is even more delicate if you are picking the observing frequency at which to image steep-spectrum extended radio emission using a *given* VLA configuration. The combined effects of a steep spectrum and changing angular resolution can make such emission *much* harder to detect with a given VLA configuration at the higher frequencies. For example, suppose that an extended emission region has a peak intensity of 1 mJy per `CLEAN` beam area in the VLA's **A** configuration at 20 cm—a 10σ detection would be made in 10 minutes. If the region has a ν^{-1} spectrum, the peak intensity in the **A** configuration at 6 cm would be 0.029 mJy per `CLEAN` beam area and a 10σ detection would need a week of integration!

For sources with compact flat-spectrum components *and* extended steep-spectrum emission, the dynamic range needed to image the extended structure increases rapidly with increasing frequency. Suppose that the extended emission referred to in the previous example surrounded a 5 mJy point source with a ν^0 spectrum. The dynamic range required for 10σ detection of the extended structure would be 50:1 in the **A** configuration at 20 cm. This is easy to obtain. The dynamic range required in the **A** configuration at 6 cm would be $\sim$ 1900:1, a non-trivial goal without self-calibration. At shorter wavelengths, the dynamic range requirements would be still greater but the atmospheric coherence times would likely be shorter and the self-calibration correspondingly more difficult.

10.1.2 Combinations of standard configurations

Options other than the standard (**A, B, C, D**) configurations of the VLA are available. You will need to combine observations made in more than one VLA configuration if you require a *range* of baselines that exceeds the range provided by a standard configuration.

As the ratio of the longest to the shortest baseline in a standard configuration of the VLA is about 40:1, each standard configuration can be used to image reliably up to $\theta_{\rm LAS} \approx 40\theta_{\rm HPBW}$ where $\theta_{\rm HPBW}$ is given by Equation 5 at the specified frequency. If the values of $\theta_{\rm LAS}$ and $\theta_{\rm HPBW}$ needed for your experiment do not *both* fall between $\theta_{\rm HPBW}$ and $40\theta_{\rm HPBW}$ calculated from Equation 5 for a given standard configuration and frequency, consider using more than one VLA configuration—unless you can extend the projected baseline range by observing at extreme hour-angles (where the u-v baselines may be significantly foreshortened). Without help from foreshortened baselines, observations requiring $\theta_{\rm LAS}/\theta_{\rm HPBW} > 40{:}1$ will need to be done in more than one configuration. Note however that some observations with $\theta_{\rm LAS}/\theta_{\rm HPBW} < 40{:}1$ may also need more than one configuration—for example, if the optimum $\theta_{\rm HPBW}$ falls mid-way between two resolutions given by allowed values of n and ν_0 in Equation 5.

When mixing standard-configuration observations to extend the range of angular scales that can be imaged, compute the bandwidths and total integration times for the different configurations separately. You will not need to spend as long a total integration time in compact configurations as in the more scattered ones, especially if you can use wider bandwidths in the compact configurations. A reasonable approach is to aim for constant surface-brightness sensitivity in observations in different configurations that will be combined to make a single image. But if possible you should also distribute the observing in the more compact configurations over at least 4 hours in hour-angle, to minimize gaps in the u-v coverage. If you leave gaps in the u-v plane by doing all the compact-configuration observing in one "scan", your images may be limited by "rumble" from poor sampling on large angular scales, rather than by sensitivity. Spreading a small amount of observing time around in hour-angle to improve the u-v coverage may be impossible if you are observing only one source, however. It is much easier to optimize a project in which several sources with similar imaging requirements can be time-shared in the more compact configurations. Otherwise, it may be necessary to collect more data in the compact configurations than sensitivity alone requires, just to sample the inner u-v plane adequately. If you do this, you should expect to reweight the short-baseline data to optimize the final synthesized beamshape and signal-to-noise together—the optimum weighting can be found empirically once the data are in hand.

10.1.3 Hybrid configurations

"Hybrid" configurations occur during reconfigurations, when the arms of the VLA may either be of different length, or have a non-standard assortment of long and short baselines. Hybrid configurations with long North arms are regularly scheduled. They are useful when imaging regions south of $\delta \approx -15°$, where the north–south extent of the u-v coverage of the standard configurations is seriously foreshortened by projection. Figures 4 and 5 compare the u-v coverage for the **B** configuration at $\delta = -40°$ with that of a hybrid configuration whose East and West arms are in the **B** configuration but whose North arm is in the **A** configuration. The baselines to the longer North arm fill in a region around the v-axis that is left empty by the standard **B** configuration. This **BnA** hybrid is available briefly about every sixteen months, during a reconfiguration from **A** to **B**. Similar **CnB** and **DnC** hybrids are scheduled between the appropriate reconfigurations.

10.1.4 Sub-arrays

"Sub-arrays" are nonstandard configurations obtained by breaking the VLA into smaller arrays that are devoted to different observing programs at the same time. The use of sub-arrays is generally not as efficient as time-sharing the entire VLA. The number of interferometer pairs in a sub-array is $N(N-1)/2$ where N is the number of antennas in the sub-array. Sub-arrays with 13 and 14 antennas therefore have 78 and 91 interferometers respectively, whereas a 27-antenna standard configuration has 351. An hour of observing in which two such sub-arrays each perform different tasks therefore produces 169 interferometer-hours of data. In contrast, two half-hours of observing, with the full VLA devoted to each task in turn, produce 351 interferometer-hours of data. Dedicating

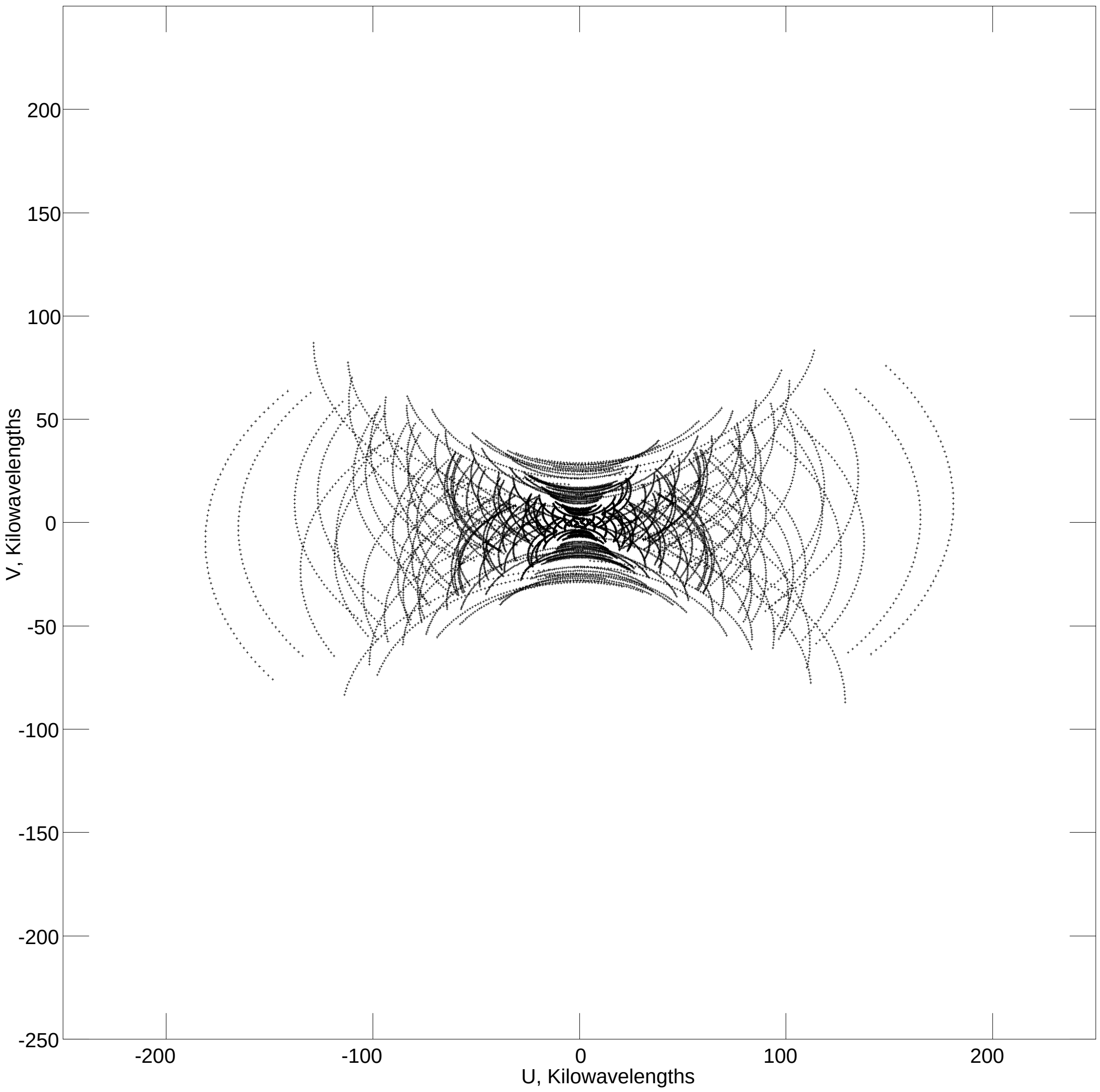

Figure 4: The u-v plane coverage at 4.9 GHz for full synthesis of a source at $\delta = -40°$ with the VLA in the **B** configuration.

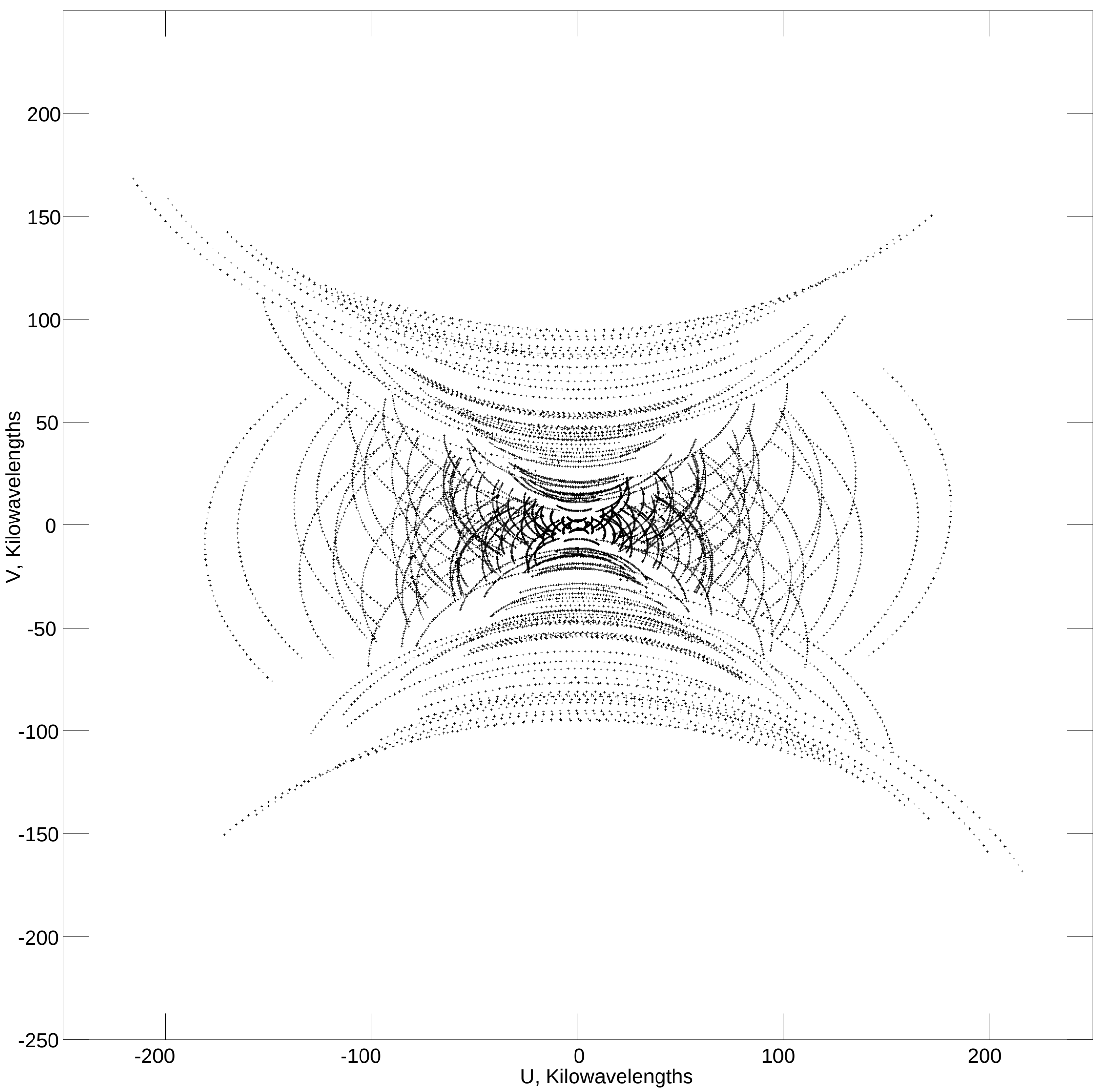

Figure 5: The u-v plane coverage at 4.9 GHz for a full synthesis of a source at $\delta = -40°$ with the VLA in the **B** configuration on the East and West arms, but in the **A** configuration on the North arm (the BnA hybrid).

Table 1: VLA Observing Frequencies

Frequency Range	Band Name	System Temperature	Antenna Efficiency
0.298 to 0.345 GHz	P Band (90 cm)	150–180	0.40
1.25 to 1.74 GHz	L Band (20 cm)	37–75	0.51
4.25 to 5.10 GHz	C Band (6 cm)	44	0.65
7.55 to 9.05 GHz	X Band (3.6 cm)	34	0.63
14.25 to 15.7 GHz	U Band (2 cm)	110	0.52
21.7 to 24.5 GHz	K Band (1.3 cm)	160–190	0.42
$\sim$40 to $\sim$50 GHz	Q Band (7 mm)	90–140	0.20

two roughly equal sub-arrays to different tasks thus reduces the amount of information gathered by a factor of about two, compared with time-sharing the whole VLA between the two tasks. This loss of information manifests itself as poorer sensitivity and u-v sampling in the sub-array data. The use of sub-arrays is therefore generally undesirable unless you need *strictly* simultaneous observations of strong sources at several frequencies (e.g., to measure instantaneous spectra of rapid variables) or to study many compact sources quickly with only modest demands on sensitivity and dynamic range (e.g., for astrometry of strong sources).

10.1.5 "Scaled" configurations

Returning to Equation 5, note that the scaling factor between "adjacent" VLA configurations (e.g., **B** and **C**) is ~ 3.3. The scaling is inexact because the North arm uses some non-scaling antenna locations in the **A** and **D** configurations. This scaling factor is near the ratios between the default VLA frequencies at 20 cm and 6 cm and between those at 6 cm and 2 cm. The VLA therefore has *similar* resolutions at 20 cm in the **A** configuration, at 6 cm in the **B** configuration, and at 2 cm in the **C** configuration. (Such rough three-frequency scalings also apply for the **B**, **C**, and **D** configurations, of course.) These scalings make the VLA a powerful tool for studying the frequency-dependence of extended emission without changing the angular resolution.

10.2 Frequency Selection

Table 1 lists the operating bands and other characteristics of the VLA receivers. (The upper and lower frequency limits are those where the sensitivity has fallen to half its maximum value, except at Q Band where these are still being determined.)

Note that a *range* of system temperatures is given for the extreme bands. At P Band, the range includes the contribution of nonthermal emission from the Milky Way—the lower value applies far from the galactic plane. At L Band, the range includes pickup of radiation from the ground at low elevation—the sensitivity decreases by about one-third at 30° elevation, one-half at 15° elevation. At K and Q Bands, the system temperatures are increased at low elevations by atmospheric emission, and are weather-sensitive (wet conditions are worse than dry).

The VLA continuum system lets you observe at two independent sky frequencies within each "band". This capability can be used to increase sensitivity, to fill in the u-v plane more densely by crude "bandwidth synthesis" or to study spectral or Faraday depth changes in your source across a "band" (the latter being especially worthwhile across the 'L' Band because the Faraday effect scales with λ^2).

Interference

Interference is rarely detected or suspected above 1.8 GHz at the VLA. It is a dominant factor in choosing a continuum observing frequency within L Band (1.25 to 1.74 GHz), particularly when

Table 2: L Band RFI at the VLA

Frequency	Avg. Flux	Pk. Flux	Source	Comments
1277 MHz	12	20	Aerostat Radar	Sometimes absent
1286	2	5	Farmington Radar	Other weak lines nearby
1300	2	5	Internal RFI	
1310	100	100	ABQ Radar	
1330	45	80	ABQ Radar	Sometimes absent
1381	3	100	GPS L3 IONDS	On $<$ 3% of the time
1400	60	60	Internal RFI	
1429-1435	15	130	Military	Four separate lines
1444,1453	5	$>$ 100	Hi altitude balloons	NASA/NSBF
1465*	6	8	Alias of 1735 MHz	
1486*	15	20	Alias of 1714 MHz	
1500	2	5	Internal RFI	
1510*	5	40	Alias of 1690	
1515	15	$>$ 100	Balloon, Alias of 1685	
1520*	9	30	Alias of 1680	
1525*	6	$>$ 100	Balloon, Alias of 1675	
1530-1544	$>$ 130	$>$ 200	INMARSAT	Many 'lines'
1557-1567	10	20	GPS Sidelobe?	Wide spectrum
1570-1580	$>$ 500	$>$ 500	GPS	Wide spectrum
1584-1598*	20	20	Alias of GLONASS	
1600	120	120	Internal RFI	
1602-1616	$>$ 500	$>$ 500	GLONASS	Many separate 'lines'
1620	80	300	?	
1625*	15	20	Aliased GPS carrier	
1650	13	25	Internal RFI	
1678-1698	50	100	Radiosondes, satellite	>6 variable 'lines'.
1710	10	10	?	
1714	$>$ 500	$>$ 500	Forest Service	
1725	10	10	" "	
1730	25	25	" "	
1735	$>$ 100	$>$ 100	Forest Service	

using non-standard frequencies (e.g., when seeking to observe at the opposite edges of the band to determine Faraday rotation parameters).

As spectroscopists do not have freedom to choose center frequencies for their projects, L Band interference may determine whether a given H I or OH line experiment is possible. There is self-generated interference throughout L Band at the VLA, mainly at the harmonics of 50 MHz; this internal interference should be below the noise in any continuum image made with an IF bandwidth $\Delta\nu > 6.25$ MHz, but can be a serious problem for spectroscopy. Extragalactic H I observations are also particularly vulnerable to external interference because the red shift moves the line towards the domain of mobile communications systems. Galactic OH observations clash with satellite navigation systems. Before using any non-standard frequency below 2 GHz, consult with VLA staff (particularly Bill Brundage, the VLA frequency coordinator) for advice and lore based on recent observers' experiences. Table 2 lists the more persistent L Band interfering signals. An archive of recent L Band interference surveys is kept at `http://www.nrao.edu/doc/vla/interference/` .

The asterisked signals are aliased, i.e. they originate from RFI at another frequency but appear

Table 3: Recommended Combinations for L Band

BW	No RFI Expected	Weak/Occas'l RFI	"Tolerable" RFI
50 MHz	none	1365,1435,1465,1485	1335,1385,1415
25MHz	1343 – 1347 1353 – 1387 1413 – 1417 1663 – 1665	1290 – 1297 1453 – 1470 1503 – 1517 1637.5	many See Table 2

Table 4: Observe names of L-band "Standard frequencies"

`Observe` Name	AC Center Frequency	AC Bandwidth	BD Center Frequency	BD Bandwidth
LL	1464.9	50	1385.1	50
L1	1364.9	50	1435.1	50
L2	1515.9	25	1365.1	25
L3	1515.9	25	1435.1	25

at the listed frequency via defects in the VLA's frequency conversion system. A new frequency conversion system has been prototyped and should be fully installed by mid-1996. The signal strengths estimated in Table 2 are appropriate for the **D** configuration, and should be considerably reduced in the wider configurations—an attenuation of ~100 may be expected in the **A** configuration due to fringe phase winding.

Between 1220 and 1250 MHz, very strong broad-band RFI is always present (apparently due to satellite and radar transmissions). It may however be possible to observe in selected, narrow bandwidths in this region. Between 1435 and 1530 MHz, aeronautical telemetry from White Sands Missile Range will occasionally, and unpredictably, affect observing.

It may be possible to observe in the presence of RFI if (a) the RFI is not strong enough to cause serious gain compression in the front-end amplifiers, and (2) it is kept out of the correlator by a narrow back-end filter.

Table 3 may help you choose center frequencies and bandwidths that are likely to result in good data. There are very few good combinations for 50 and 25 MHz bandwidths. Table 4 shows what are "statistically" the best frequencies to use at L Band with the given bandwidths.

10.3 VLA Bandwidth Selection

Users of extremely narrow bandwidths should be aware that when observing in continuum mode the VLA bandwidths narrower than 6.25 MHz suffer large closure errors because the quadrature networks do not work well. If such narrow bandwidths are essential for your observations, consider observing with the spectral-line system, where these problems are avoided. Unfortunately, the VLA spectral-line system is not a panacea for eliminating chromatic aberration: it cannot support continuum polarimetry in all 4 "IFs".

Chromatic aberration effects at the VLA are well estimated by the expressions given by Bridle & Schwab (1989) for a square bandpass and Gaussian tapering in the u-v plane. In the regime $(0 < \beta \leq 1)$ where the amplitude reduction for a point source is moderate, the exact expression for the reduction (their Equation 13–23) can be approximated by

$$\frac{I}{I_0} \approx 1 - \frac{1}{3}\left(\frac{\gamma \Delta\nu \theta}{2\nu_0 \theta_{\mathrm{HPBW}}}\right)^2 + \frac{1}{10}\left(\frac{\gamma \Delta\nu \theta}{2\nu_0 \theta_{\mathrm{HPBW}}}\right)^4 , \tag{6}$$

using the standard expansion for the error function, erf, at small values of its argument.

10.4 VLA Averaging Times

The on-line visibility averaging time τ_{a} at the VLA may be set to any multiple of 1.67 sec, but the even multiples are preferable, for reasons associated with the VLA phase switching system. In practice, averaging for only 1.67 sec may give large ($\sim$ 10 mJy) correlator offsets, so the shortest τ_{a} recommended for all applications is 3.3 sec. The "default" values of the on-line visibility averaging time τ_{a} at the VLA are 10 sec for the **A** and **B** configurations and 30 sec for the **C** and **D** configurations.

The effects of the on-line averaging are permanent, because the averaged data are written to the archive tape created by the on-line system. It is therefore important to choose an on-line averaging time that limits time-averaging distortions to acceptable values, and is shorter than the expected atmospheric coherence time (provided the hardware and computer restrictions permit such a choice—spectroscopists must note Table 9). Longer averaging times may be used off-line, e.g., once the data have been calibrated.

For Gaussian tapering in the u-v plane, the intensity reduction due to a finite averaging time τ_{a} is given by Bridle & Schwab's Equation 13–39 with $\alpha = \gamma^2/\pi^2$, which we may write as

$$\frac{I}{I_0} \approx 1 - \frac{\gamma^2}{12}\omega_e^2 \tau_{\mathrm{a}}^2 \left(\frac{\theta}{\theta_{\mathrm{HPBW}}}\right)^2 . \tag{7}$$

Spectroscopists should use Equation 7, with values of I/I_0 that are acceptable for their experiment, to determine the maximum acceptable averaging time.

Continuum observers may wish instead to use an averaging time $\tau_{\Delta\nu}$ that produces the *same* intensity reduction for a source near the pole as does an IF bandwidth $\Delta\nu$. This can be approximated (for small intensity reductions) by equating the terms in $\theta^2/\theta^2_{\mathrm{HPBW}}$ from Equations 6 and 7, obtaining

$$\tau_{\Delta\nu} \approx \frac{\Delta\nu}{\omega_e \nu_0} = 1.375 \times 10^4 \, \frac{\Delta\nu}{\nu_0} \mathrm{sec} . \tag{8}$$

Equation 8 gives a reasonable criterion for the maximum averaging time τ_{a} that should be used with an IF bandwidth $\Delta\nu$ for continuum observations at observing frequency ν_0. Notice that $\tau_{\Delta\nu}$ does not depend on VLA configuration or on $\theta_{\max}$, owing to the first-order similarities between the chromatic aberration and time-average smearing for a polar source. There is an intuitive basis for Equation 8: for a polar source, time averaging smears the visibilities over an *angle* $\omega_e \tau_{\mathrm{a}}$ in the u-v plane so its effects scale as $\sqrt{l^2+m^2}\,(\omega_e \tau_{\mathrm{a}})$, whereas those of bandwidth smearing scale as $\sqrt{l^2+m^2}\,(\Delta\nu/\nu_0)$.

You may have to exceed the value of $\tau_{\Delta\nu}$ calculated from Equations 7 or 8 because the VLA's on-line system cannot provide averaging times less than 1.67 seconds in any of the normal observing modes. Note also that the VLA on-line system averages all baselines with the same τ_{a}. If the calibrator observations are only a few minutes each (as is often the case at low frequencies), averaging times longer than 1 min are undesirable because they permit only crude editing of the calibrator data. τ_{a} is also limited in many cases by the size of the final data set, especially for multiconfiguration continuum syntheses, or multichannel—continuum or spectral line—observing (Table 9). If storing the data set requires much more than the average disk space available per user in the off-line computers, data processing (and/ or life with one's colleagues) becomes difficult. Averaging times τ_{a} are sometimes set longer than would otherwise be desirable, just to avoid such "excessive" data volumes. Most VLA continuum observing is done with 10 sec $< \tau_{\mathrm{a}} <$ 1 min because of these constraints. For line work, Table 9 gives the limits that are imposed by the correlator.

Table 5: Theoretical R.m.s. Noise on Images Made with 27 VLA Antennas*

Wavelength	92 cm	20 cm	6 cm	3.6 cm	2 cm	1.3 cm
Band Designation	P	L	C	X	U	K
ΔS (1 sec, 1 MHz), Jy	1.87	0.38	0.35	0.29	1.14	2.0
Bandwidth $\Delta\nu$, MHz	3	50	50	50	50	50
R.m.s. in 5-min snapshot, mJy/beam	2.1	0.12	0.11	0.09	0.35	0.61
R.m.s. in 12-hr synthesis, mJy/beam	0.18	0.010	0.009	0.007	0.029	0.051
*Two IFs, natural weighting. For uniform weighting, multiply entries by ~1.5						

10.5 The Primary Beam

To the accuracy needed when planning observations, the primary beam of the VLA antennas can be taken to be a Gaussian with FWHM equal to $90\lambda_{\rm cm}$ arcsec or $45/\nu_{\rm GHz}$ arcmin. If you must image a source, or a field of view, that is significantly larger than the FWHM of the VLA primary beam, then you should plan to make a mosaic from a number of pointings (see Lecture 14).

In standard VLA software, the primary beam correction ($1/\mathcal{A}$, Lecture 2) is modeled by a power law expansion of the form $\frac{1}{\mathcal{A}} = \sum a_i X^{2i}$ where $X = \theta_{arcmin}\nu_{GHz}$ and the coefficients are $a_0 = 9.920378 \times 10^{-1}$, $a_1 = 9.956885 \times 10^{-4}$, $a_2 = 3.814573 \times 10^{-6}$, $a_3 = -5.311695 \times 10^{-10}$, and $a_4 = 3.9809630 \times 10^{-12}$ (Napier and Rots 1982). This correction is usually not applied at small values of X for which the Napier–Rots expansion gives $\mathcal{A} > 1$. It is not well determined at large values of X for which $\mathcal{A} < 0.15$.

10.6 Sensitivity

Table 5 gives the theoretical r.m.s. noise on I and P images made at the VLA without tapering, using 27 antennas and the maximum interference-free continuum bandwidths, for integration times typical of "snapshots" (see Section 10.7 below) and of more complete syntheses. (Interference normally restricts observations at 92 cm to a 3 MHz bandwidth.)

Note that some parameters that affect these sensitivities improve with time as a result of receiver upgrades, improved feed designs, adjustment of the antenna surfaces after holography, etc. The *VLA Observational Status Summary* reports relevant system parameters at least once per year. Check the most recent version of this when planning a VLA proposal. It is available over the World-Wide-Web at:
`http://www.nrao.edu/doc/vla/obstatus/vlas/vlas.html`.

10.7 "Snapshot" Mode

The VLA's "Y" layout gives an *instantaneous* synthesized beam with a respectable shape and side-lobe level. This makes it possible to do interesting science with only brief observations if the targets are both bright and compact. In what follows, I consider a single "snapshot" to be an observation of <5 minutes' duration. Snapshots of <1 minute duration may even be appropriate if you want to image many (>1000) fields that are near to one another on the sky (so that antenna drive times are also short) and it does not matter if the occasional observation is abbreviated or even lost. Such observing can be ideal if you want to study the statistical properties of a large sample of small, bright sources (and also to overdose on synthesis image processing!).

Note that two extensive snapshot surveys are in progress using the VLA at L Band: the whole sky is being observed in the **D** configuration (the NVSS project), and the Sloan survey region (initially) is being observed in the **B** configuration (the FIRST project). The accumulating data

Table 6: Approximate Values of $\theta_{\rm LAS}$ for a Single Snapshot

	A	**B**	**C**	**D**
92 cm	$1.5'$	$4.5'$	$15'$	$35'$
20 cm	$20''$	$1'$	$3.5'$	$7.5'$
6 cm	$5''$	$18''$	$1'$	$2.2'$
3.6 cm	$3.5''$	$10''$	$30''$	$1.2'$
2 cm	$2.0''$	$6''$	$20''$	$45''$
1.3 cm	$1.0''$	$3.5''$	$13''$	$30''$
7 mm	$0.7''$	$2.2''$	$6.5''$	$22''$

from these two surveys are in the public domain and should be checked for overlap with any proposal for L-band snapshots in the **B**, **C** or **D** configurations.

10.7.1 Limitations of "snapshot" mode

The clearest limitation of snapshot observing is sensitivity (see Table 5); snapshot mode is suitable only for bright sources. Below 2 GHz and especially at P Band, the high sidelobe levels of snapshot beams exacerbate the problems created by confusing sources. Snapshots of fields near the galactic plane using the more compact VLA configurations at lower frequencies are frequently dominated by sidelobe clutter from confusing sources rather than by the noise that is quantified in Table 5. These problems are less severe above 2 GHz because of the smaller primary beam and the typical source spectrum (see Section 10.9on "Confusion" below).

The second limitation of snapshot observing is the restricted angular size scale $\theta_{\rm LAS}$ over which the *u*-*v* coverage of a snapshot (e.g., Fig. 6) satisfies the sampling theorem and thus permits reconstruction of the correct sky brightness distribution. Table 6 estimates this limitation for snapshots on the meridian in the standard VLA configurations and frequencies, averaged over all declinations. Larger structures can be imaged by combining a few snapshots taken at different hour angles.

Polarization calibration may be difficult for short snapshot programs; it is not easy to verify the instrumental polarization calibration for a program whose total observing time is only a few hours, as this calibration requires at least three observations of a calibrator spanning a change in parallactic angle χ of $\Delta\chi \geq 90°$ (see Lecture 7). Snapshooters interested in polarimetry should ensure that suitable polarization calibration is possible when designing their program, by giving attention to its LST range.

Snapshots are most effective when all sources are observed within about 2 hours of the meridian. At larger hour-angles, foreshortening of the array leads to poorer sampling of the *u*-*v* plane, elliptical synthesized beams, etc.

The time taken to calibrate a snapshot data set is determined mainly by the total observing time. Snapshot programs require the same calibration effort as simple synthesis programs of the same total duration. The image construction, deconvolution and display steps of snapshot observing can require large amounts of computer time and your time, however. As a snapshot image of a given target may be as large as a full synthesis image of the same field, snapshot programs also make heavy demands on disk storage. This can be especially true for snapshots made in the more compact configurations below 2 GHz, which are particularly prone to degradation by sidelobe clutter from confusing sources.

10.7.2 Multiple snapshots versus extended snapshots

Snapshots require phase stability only for the duration of the individual snapshot. There is therefore some debate over whether (for example) an observation requiring 15 minutes of integration time

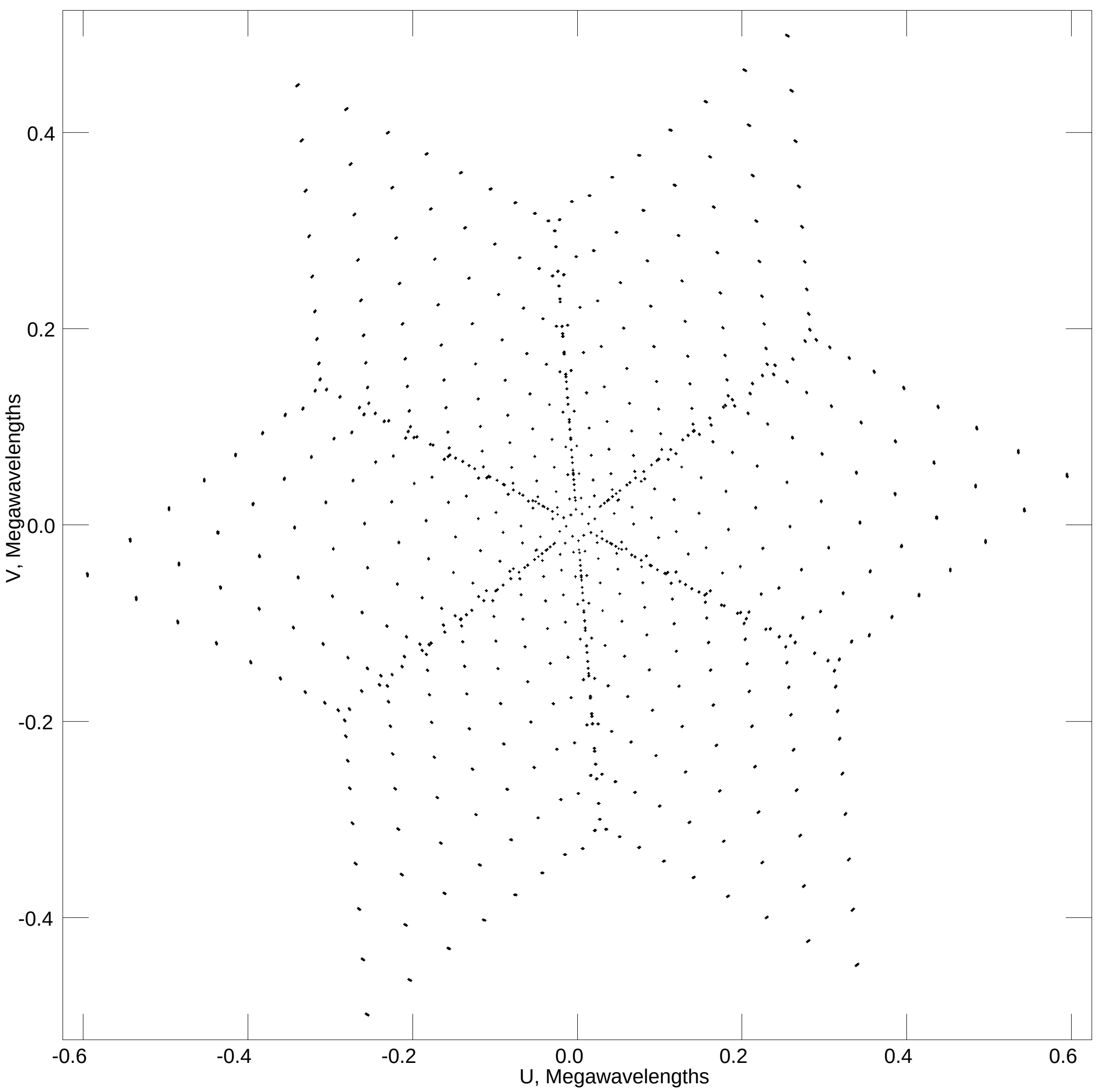

Figure 6: The u-v plane coverage at 4.9 GHz for instantaneous sampling of a source at $\delta = 30°$ and hour-angle 0^{h} with the VLA in the **A** configuration.

Table 7: Maximum Channels in VLA Spectral Line Modes

	Without Hanning		With Hanning	
Bandwidth (MHz)	Channels	Separation (kHz)	Channels	Separation (kHz)
0.195313	512	0.381	256	0.763
0.78125	512	1.526	256	3.052
1.5625	512	3.052	256	6.104
3.125	256	12.207	128	24.414
6.25	128	48.828	64	97.656
12.5	64	195.313	32	390.625
25	32	781.25	16	1562.5
46	16	3125	8	6250

$t_{\rm int}$ is better made as one continuous 15-minute observation or by combining the data from three separate 5-minute snapshots. A single 15-minute observation may give better dynamic range, because ionospheric or tropospheric phase gradients in the form of "wedges" may calibrate out of a single short observation, leaving only a position shift. In contrast, three shorter observations that are more dispersed in time and calibrated on a long calibrator cycle may encounter different wedges and so combine to give an image with poorer final dynamic range, unless self-calibration (Lecture 9) can be used. There are therefore some circumstances in which a single observation is preferable, as well as being easier to schedule.

The advantages of combining data from several shorter snapshots are (a) greater protection against total loss of the data for a given source through equipment failures or short-term bad weather, and (b) more even sampling of the *u*-*v* plane than in a single extended snapshot. Multiple snapshots are particularly useful when observing at wavelengths of 18 cm and longer in the **C** and **D** configurations, as they allow better imaging of confusing sources that may otherwise limit the achieved dynamic range (see Section 10.9below). The single extended snapshot may be better for observations that must be made at low elevations, where phase "wedges" are more likely to arise, and if self-calibration cannot be used. This may be particularly true for observations of weak or complex low-declination sources for which the total hour-angle coverage is anyway limited by the short time that a given source is above the horizon.

10.8 Constraints on Spectral Line Observing

The VLA correlator has enough chips to produce 16 complex frequency channels at the nominal "50 MHz" (46 MHz) bandwidth. Halving the total bandwidth allows the chips to be "time-shared" so that the number of channels is doubled. This total bandwidth halving and time-sharing can be continued to a maximum of 512 channels, at which point further halvings of the total bandwidth leave the number of channels at a maximum of 512. Table 7 summarizes the resulting channel number and channel width options for a single IF, with and without on-line Hanning smoothing. Hanning smoothing to reduce the Gibbs phenomenon is strongly recommended for all observations that require high spectral dynamic range; it may be applied either on-line or off-line.

The above total numbers of channels may also be split evenly among two, or four, IFs. For example, if an observation is set up at 12.5 MHz total bandwidth with 2 IFs and no on-line Hanning smoothing, there will be 32 channels in each of the two spectra (i.e., 32 per spectrum for a total of 64 as shown in the table). The splitting among the IF channels is selected on the //DS input "card" by specifying the correlator "mode". Note that the first channel ("channel 0") of each IF contains the complex average of the central 75% of the band that the correlator has available (even if not all

Table 8: VLA Spectral Line Correlator Modes

Mode	Polarimetry?		Number
	Circ	Lin	and ID of IFs
1A	No	No	1 A
1B	No	No	1 B
1C	No	No	1 C
1D	No	No	1 D
2AB	No	No	2 A,B
2AC	Yes	No	2 A,C
2AD	No	No	2 A,D
2BC	No	No	2 B,C
2BD	Yes	No	2 B,D
2CD	No	No	2 C,D
4	Yes	No	4 A,B,C,D
4PA	Yes	Yes	4 A,C
4PB	Yes	Yes	4 B,D

Table 9: VLA Averaging Time Restrictions

Channels	Minimum (sec)
1	3.33
8	3.33
16	3.33
32	3.33
64	3.33
128	6.66
256	10
512	20

of that band has been selected).

Table 8 summarizes the VLA spectral line correlator modes.

Each mode in which the correlator can provide spectral line data is characterized by a number followed by zero, one or two letters. The number gives the number of spectra produced, the letters describe which IF channels (A,B,C,D) are in use. Recall that A and B are right circularly polarized, C and D are left circularly polarized, and that A and B are at one sky frequency, B and D another.

The single-channel modes are known as 1A, 1B, 1C and 1D. These produce only one spectrum but with the highest spectral resolution at any bandwidth.

The dual-channel modes are 2AB, 2AC, 2AD, 2BC, 2BD and 2CD. None of these will measure linear polarization, but 2AC and 2BD can determine circular polarization.

The four-channel modes are known as 4, 4PA and 4PB. The first provides spectra for all 4 IF channels and can measure circular, but not linear, polarization (no cross-correlations between the circular modes are produced). 4PA mode produces all four possible correlations from the A and C channels — AA, AC, CA and CC – with a spectrum for each. 4PB provides the analogous output for the B and C channels. For these linear-polarization-capable modes, the descriptor 4 is often omitted.

Table 9 gives the averaging time restrictions that are imposed by the VLA correlator.

The *Spectral Line Users' Guide* (available on the World-Wide-Web at `http://www.nrao.edu/doc/vla/obstatus/splg1/splg1.html`) has further information on the VLA spectral line system.

10.9 Confusion

The number of extragalactic sources N per square arc minute of sky with flux densities greater than S mJy at 6 cm can be written approximately as

$$N(>S) = 0.032 S^{-1.13} \tag{9}$$

over the flux density range that is relevant for confusion calculations at the VLA (e.g., Ledden *et al.* 1980). The corresponding expression at 20 cm is

$$N(>S) = 0.10 S^{-0.9}\,. \tag{10}$$

The analogs of these expressions for 2 cm and 1.3 cm are not known directly from measured source counts. They could be *estimated* from the 6 cm count in Equation 9 by scaling flux densities to 6 cm with an effective mean spectrum of $\sim \nu^{-0.6}$.

Images made at 20 cm will contain, on average, one extragalactic source of flux density 110 mJy closer to the field center than the $15'$ HWHM of the primary beam. The 6 cm primary beam ($4.5'$ HWHM) will contain, on average, one extragalactic source of flux density 2 mJy, the 2 cm beam ($1.85'$ HWHM) a source of < 0.1 mJy and the 1.3 cm beam ($1'$ HWHM) a source of < 0.01 mJy. At 92 cm, there is always at least one several-Jy source in the primary beam and there may be many. Individual pathological cases aside, confusion is unlikely to be a problem at wavelengths shorter than 6 cm. At 20 cm and 6 cm it may be a problem in the VLA's more compact configurations. At 92 cm it is a problem in *all* configurations.

Confusion is particularly troublesome for snapshooters using the compact configurations below 2 GHz, because the sidelobes resulting from the "snowflake" *u-v* coverage of snapshots (Fig. 6) are extensive. Images at low galactic latitudes are also more confused than those at high galactic latitudes. Snapshooters should plan to reduce their data using the ungridded subtraction algorithm (`MX` or `IMAGR` in AIPS) both because it permits imaging of multiple subfields and because it eliminates the effects of sidelobe aliasing.

10.10 Calibration Details

10.10.1 Instrumental and atmospheric monitoring

Reference sources should generally be chosen from the *VLA Calibrator List* (maintained by the NRAO staff and referenced by the `OBSERVE` program), unless you are sure that a putative calibrator is unresolved in the VLA configuration that will be used, and has a position measured in the VLA reference system to better than $0.1''$.

The length of time spent on each calibration scan should be enough to achieve a signal-to-noise (over the 26 baselines contributing to each antenna gain solution) commensurate with the required calibration accuracy. Never plan to calibrate for less than 1 minute at a time, however, as shorter calibrator scans may be lost as a result of unusually long settle-down times, etc. Significant atmospheric amplitude and phase fluctuations can occur on time scales of minutes, even at wavelengths of 6 cm and longer. When the Sun is active, *ionospheric* fluctuations will dominate at 18 cm and longer—they can also be rapid on long VLA baselines. It is completely impractical to adopt a calibrator–target–calibrator cycle that will guarantee following the fastest fluctuations of either kind. Keep in mind that *no* external referencing, no matter how rapid, can be *guaranteed* to remove atmospheric fluctuations from the data, and that time spent driving to and observing calibrators is time deleted from integration, and *u-v* coverage, on your target. You must decide for yourself how to play this particular roulette game during a given run.

Typical VLA observing programs spend from 5% to 10% of their time on calibration at the lower frequencies; more calibration may be needed at the higher frequencies where the calibrators are weaker and therefore need to be observed for longer total integration times. Calibration every 20 minutes or so will often follow the longer-term atmospheric fluctuations at 20 cm and 6 cm, especially in the more compact VLA configurations. Calibration every 10 minutes or so is safer at 2 cm and shorter wavelengths, especially if the external calibrator is within a degree or so of the target. It should not be necessary to calibrate instrumental effects more rapidly than every 30 minutes at 20 cm or 6 cm.

Finally, note the significance of the choice of the gain table interval for the VLA off-line data base created by the `FILLM` program *if you will not self-calibrate* your data. The off-line gain table interval (which you specify to the array operator at the time of the observations) sets the minimum time scale of instrumental or atmospheric fluctuations that can be corrected by an external calibration. (Self-calibration algorithms construct their own gain tables based on the integration time $\tau_{\rm sc}$ that you specify for the gain determination.) The VLA default gain table interval of 10 minutes is adequate for calibration under a stable atmosphere, but shorter intervals are often more appropriate if you will rely on external calibration.

10.10.2 VLA flux density calibration

3C 286 is the (slowly-varying) flux-density standard to which all VLA measurements are ultimately referred. If the LST range of your observing run permits, observe 3C 286 for a few minutes at each observing frequency and bandwidth combination that you use for the targets, Failing this, observe 3C 48 or 3C 147 instead (or consult with VLA staff about recent determinations of the amplitude gains of the antennas from other observations before finalizing your observing program). Do not simply take the most recent flux density for an arbitrary calibrator from the *VLA Calibrator List* . Many small-diameter sources that in this list because they are suitable for position and instrumental calibration are variable. The flux densities recorded in the *VLA Calibrator List* will rarely have been measured recently enough to determine the absolute flux-density scale for your observations; use them only to estimate the integration times needed to achieve the desired gain accuracy from your calibrator scans.

10.10.3 VLA polarization calibration

Instrumental

To calibrate the *instrumental polarizations*, observe one unresolved calibrator, whether polarized or not, *at least* three times, more often if possible. Distribute these observations to cover a range in parallactic angle χ of $\Delta\chi \geq 90^\circ$: this will separate any polarization of the calibrator from the required instrumental terms (see Lecture 7). Programs involving long ($\geq$ 4 hr) syntheses of single sources will normally be able to derive the instrumental polarization calibration from the observations of the external gain calibrator. When determining the integration time for the instrumental polarization calibration, bear in mind that the cross-polarization (leakage) terms whose relative amplitudes and phases are to be determined will likely produce false polarized intensities that are only a few percent of the flux density of the calibrator. The instrumental polarization calibration must be done at each frequency for which polarimetry is required. The most efficient way to do this is to cycle through the frequencies used for the target observations each time you point the array at the calibrator. If you omit an instrumental polarization calibration, you will be unable to determine small degrees of polarization reliably, or to deconvolve polarized extended structures properly. (Antenna-to-antenna polarization differences distort the polarization images in ways that do not satisfy the convolution theorem.)

Position Angle

To calibrate the *polarization position angle* scale, observe 3C 286 or 3C 138 at least once during your observing run at each relevant frequency. You will determine the apparent position angles of the linear polarization of these sources after you have finished observing and after calibrating the total intensity data. The difference between the apparent and the nominal values of these position angles is corrected by adjusting the phase difference between the left and right circular polarizations, using a procedure that is described in detail in the *AIPS Cookbook*. It is advisable to alert the array operator to the presence of this calibration in your program, so that the observations of 3C 286 or 3C 138 can be extended or rescheduled if necessary to avoid losing them to equipment failure. Note that this calibration is *essential* if you wish to use your polarization position angle data, e.g. to determine magnetic field directions or to measure the Faraday rotation of a source.

Ionospheric Faraday Rotation

At wavelengths of 18 cm and longer, the position angle calibration may appear to be time variable because of fluctuations in the ionospheric Faraday rotation (Lecture 7). If you will use the polarization position angle information at long wavelengths, it is worth monitoring one polarized calibrator *in the same part of the sky as your target(s)* throughout your observing, to see if its apparent position angle changes significantly. If this calibration shows that the ionospheric changes are less than about 20°, it may be satisfactory to interpolate the observed position angle changes as a function of time when you set the position angle scale by adjusting the relative phase of the left and right circularly polarized channels. If you see larger changes, especially in a calibrator some tens of degrees from your target, it may be impossible to correct for them accurately without using an ionospheric model. Unfortunately, a source of critical-frequency data that was used to estimate ionospheric models for many years at the VLA (via the `FARAD` programs) is no longer available. Until it is replaced (possibly by data from GPS systems), there is no way to repair VLA polarimetric data sets in which the ionospheric Faraday rotations are large. Observing a polarized calibrator can therefore be a "warning light" for such ionospheric Faraday rotation problems, but it does not guarantee a way to correct them. Fortunately, ionospheric effects are normally negligible above 4 GHz.

10.10.4 Self-calibration criteria

To decide whether or not you will be able to self-calibrate VLA data, use Equation 4 with $N = 27$, i.e.,

$$\phi_{rms} \approx \frac{13\Delta S}{S_{sc}\sqrt{\Delta\nu\,\tau_{\rm sc}}} \text{ degrees}\,, \tag{11}$$

to estimate the phase error in a self-calibration interval $\tau_{\rm sc}$.

10.10.5 Extreme Games I: P Band

Calibration at P Band is particularly troublesome because of confusion in the primary beam. Confusing sources contribute several Jy or more to every field of view, and the use of narrow bandwidths for interference rejection implies that these sources contribute significantly to virtually all baselines. External calibrators must therefore be chosen for their strength rather than by nearness to the interesting field of view. Calibrators with >25 Jy are preferable. Unless the calibrator is >5 Jy, you may as well attempt self-calibration using the brightest sources in the field. Self-calibration with the traditional algorithms may not work under severe ionospheric conditions, where the size of the isoplanatic patch may become smaller than that of the primary beam. Perley (1988) has listed possible P Band calibrators.

Because ionospheric Faraday rotation at P Band is large and variable, polarization calibration is extremely difficult and cannot be guaranteed unless the ionosphere is exceptionally "quiet" during an observing run.

Note also that at P Band, only the **D** configuration satisfies the conditions for imaging using a two-dimensional Fourier transform(Lecture 10) with a non-coplanar array. P Band observations in the more extended configurations must either use special-purpose software (consult Tim Cornwell) to correct for the effects of the non-coplanar baselines, or accept more approximate removal of only the strongest confusing sources in the field using `MX` or `IMAGR` in AIPS.

10.10.6 Extreme Games II: Q Band

Q Band receivers are installed on only 10 VLA antennas, whose aperture efficiencies are about 20% and are still being improved by holography and focus adjustments. The optimal layouts for these antennas during each VLA configuration are still being explored. The nominal tuning range for the receivers is 40–50 GHz, but the aperture efficiency falls by about a factor of two between 43 and 49 GHz while the system temperature increases by about a factor of two. The details of the performance across the whole band are still being investigated.

The sky opacity at Q Band is dominated by an atmospheric O_2 line at 60 GHz so it varies little with the weather; typical zenith opacities are 0.06 at 43 GHz and 0.15 at 49 GHz. Plan about 10 minutes to determine the zenith sky opacity from a total power tipping scan during your observations.

Phase coherence varies greatly from day to night. Under poor day-time conditions, phase referencing on SiO maser sources or self-calibration are essential. Under dry night-time conditions, external calibrations on time scales of 10–20 minutes are also likely to succeed.

Because of the small ($1'$) primary beam size at Q Band, accurate pointing is critical to Q Band observing and you should plan to make reference pointing observations at X Band about once an hour throughout Q Band observing. Reference pointing scans should take about 4 min. It is important to select reference pointing calibrators as close as possible to, and definitely within 30° in azimuth and elevation of, your target sources. The phase calibrator is often a good choice for the reference pointing calibrator. If possible, choose a pointing calibrator with a smaller right ascension than your target, so the target drifts through the reference pointing position during the observation. Avoid observing sources within 10° of the zenith.

As the Q Band system on the VLA is relatively new and the NRAO staff and users are still gaining experience with it, information about Q Band performance and optimal observing strategies is changing rapidly. It is therefore a good idea to consult the Q Band page on the World-Wide-Web (`http://www.nrao.edu/doc/vla/html/Qband/qband.shtml`) for updated information before finalizing Q Band observing plans.

10.11 Observing Proposals

VLA observing proposals are refereed outside the NRAO before being considered by the scheduling committee. To receive high priority, the scientific goals must favorably impress a panel of external referees who read a hefty batch of such proposals at each competition. A "highly-placed source who wishes to remain anonymous" notes that more concisely-written proposals are more likely to be refereed favorably, all else being equal. A good proposal will make it crystal clear what astrophysical questions are being asked, and how the specific measurements that are being proposed will answer them. It will also show that you chose the array configurations, observing frequencies, total observing time etc. carefully to optimize your chance to reach your scientific goals.

Before you begin writing a proposal, you should check whether any of your target sources have already been observed at the VLA. The NRAO routinely archives the raw (uncalibrated) visibility data from all VLA observations. General access to these data is restricted for 18 months after the end of the associated observing program. Thereafter, the raw data are available to any interested scientist. Apart from the large-scale NVSS and FIRST L Band surveys that are now in progress, calibrated and processed data remain the property of the original observer so are not automatically

(16) Number of sources __ (If more than 10 please attach list. If more than 30 give only selection criteria and LST range(s).)

(17) NAME	Epoch: 1950 ○ 2000 ○ RA hhmm Dec $\pm$ xx.x°	Config.	Band (cm)	Band-width (MHz)	Total Flux		Largest angular size	Required rms (mJy/bm)	Time requested (hours)
					line (Jy)*	cont. (Jy)			

*this should be the total flux at the peak of the line

Notes to the table (if any):

Figure 7: Source Table from VLA Proposal Cover Sheet

indexed or archived at the VLA. They may however be available from that observer, or even be on one of the NRAO CD-ROMs.

Catalogs of the observed sources, including relevant instrumental parameters, can be obtained by reading the *Cumulative Observation List* from the *VLA Home Page* at (`http://www.nrao.edu/doc/vla/html/VLAhome.shtml`), or from the MS-DOS PC database program `VLASORS` (see Section 10.12.1below). The *VLA Archive Database* is a growing, but still incomplete, segment of this list that can be queried over the World-Wide-Web using an HTML forms interface (`http://info.aoc.nrao.edu/doc/vladb/VLADB.html`, also accessible from the VLA Home Page). If you decide that the major parameters of an earlier observation are also appropriate for your work, you may either contact the original observers to use their calibrated data, or request use of the uncalibrated data from the VLA archive. Watch the *NRAO Newsletter* and the *VLA Home Page* for updates about the archive and associated software.

When writing the proposal, think about your calibration strategy in detail, as well as the target source observations. The total time you request should include all the on-source integration time that you need, plus enough time for any and all calibrations that you will do. Depending on the project, calibration time may need to be from 10% to 50% of the total. Filling out items 16 and 17 on the proposal cover sheet (Fig. 7) for each target, or for typical targets, will lead you to consider the issues discussed here. Your entries should show that the proposal is well suited to the requested configuration(s).

VLA observations may be scheduled for as little as half an hour at a time or for as long as several days. The median time that is scheduled varies from configuration to configuration, but is typically 6–8 hrs. Observations that are much longer than this median time will generally be harder to come by than observations that are much shorter, but there are no hard guideline in either direction. Recognize however that there is always more observing time proposed than can be scheduled, and that proposals for longer-than-usual observing times will probably have to generate more-than-usual scientific excitement to get as much time as they ask for. There is generally more pressure for observing time in the LST ranges of popular targets such as the Galactic Center and the Virgo Cluster. The VLA all-sky surveys are also (temporarily) affecting the availability of observing time for other programs: night-time observing in the **D** configuration will be in short supply in the Summer of 1996, and LST's from 0700 to 1730 hrs will be in short supply in the **B** configuration for late 1995 and early 1977. Table 10 gives the projected long term configuration schedule (note that this is subject to change—updates are published regularly in the *NRAO Newsletter* , the *AAS*

Table 10: Long term VLA Configuration Plan

	Q1	Q2	Q3	Q4
1996	C	D	D	A
1997	B	C	C,D	D
1998	A	B	C	C,D
1999	D	A	B	C
2000	C,D	D	A	B

Table 11: Near Term VLA Proposal Deadlines

Observing Dates	Config	Proposal Deadline
28 Jun 1996 - 30 Sep 1996	D	01 Feb 1996
18 Oct 1996 - 30 Dec 1996	A	03 Jun 1996
10 Jan 1997 - 27 Jan 1997	BnA	01 Oct 1996
31 Jan 1997 - 12 May 1997	B	01 Oct 1996
23 May 1997 - 09 Jun 1997	CnB	03 Feb 1997

Newsletter and in the *VLA Observational Status Summary* .

Proposals should be sent to the NRAO well before the deadline for the desired configuration(s). Table 11 lists the upcoming proposal deadlines and the observing periods and configurations to which they apply.

Proposals can be submitted in two ways (note that FAXes are not acceptable):

1. via paper mail to the NRAO Director (Dr. Paul A. Vanden Bout, National Radio Astronomy Observatory, 520 Edgemont Road, Charlottesville, Virginia 22903-2475) using the NRAO proposal form, or

2. by E-mail to `propsoc@nrao.edu` as a Postscript file (based on an NRAO TEX template that generates the proposal form).

Detailed instructions for submitting VLA proposals can be found on the World-Wide-Web under the *VLA Home Page* (`http://www.nrao.edu/doc/vla/html/VLAhome.shtml`) or at `http://info.cv.nrao.edu/html/headquarters/tel-vla.html`; or by contacting Joanne Nance in Charlottesville (`jnance@nrao.edu`, 804-296-0323).

You need not wait until the deadline for a particular configuration before submitting a proposal. You might submit a proposal for an earlier deadline for two reasons—(a) the pressure of proposals for a given configuration influences the length of time that the VLA is scheduled to spend in the configuration, (b) early submission may let you respond to unfavorable comments from the referees before the scheduling committee assigns time for the requested configuration(s).

10.12 PC Software

Two PC-based software packages that are useful when planning VLA observing can be obtained by anonymous-ftp from `ftp.aoc.nrao.edu` or on diskettes from Theresa McBride at the NRAO in Socorro (`tmcbride@nrao.edu`, 505-835-7245).

10.12.1 VLASORS

This self-documenting database query program will search either for calibrators in the *VLA Calibrator List* or for sources from the observation archive list. The *Calibrator List* may be searched by source name, frequency, flux density, or area of sky. The archive list may be searched by source name, frequency, position, proposer or project number. `VLASORS` can be run on any MS-DOS PC with a hard disk. The archive of all observations with total integration times longer than one hour requires 4 Mbytes of hard disk storage. The file of all observations requires 8 Mbytes. `VLASORS` can be obtained by anonymous-ftp from the `/pub/vlasors` directory—get the `read.me` file first for detailed instructions.

You can also search the *VLA Calibrator List* from the World-Wide-Web by linking to `http://www.nrao.edu/~gtaylor/calib.html`.

10.12.2 VLAPLAN and VLAUVPL

`VLAPLAN` (Bridle 1994) is a menu-driven MS-DOS PC program that can help you plan continuum, spectral line, or bandwidth synthesis observing strategies for the VLA using the approaches and formulae described in this lecture. The calculations are organized into several self-documenting spreadsheet-like screens. These screens let you explore the consequences of different parameter choices quickly. They also offer advice on how to meet your imaging specifications, and warn of serious parameter conflicts. `VLAPLAN` also plots context-sensitive graphs of the bandwidth and time average smearing effects, of the primary beam correction, and of Gaussian source visibility functions. L Band users are also warned of any persistent interfering signals within their chosen bandpass. `VLAPLAN` can be run as a (frozen) stand-alone program, or as a (modifiable) spreadsheet template under Lotus *1-2-3* or under Borland *Quattro Pro* in any of its 1-2-3-compatible incarnations. It is available by anonymous-ftp from `ftp.aoc.nrao.edu`, in the `pub/vlaplan` directory—read the file `vlaplan2.doc` first for detailed instructions and for update information.

`VLAPLAN` recommends VLA configuration(s) for your observing, including multiple configurations where appropriate. It chooses the most compact configuration based on the observing frequency, the largest angular size and declination of your source. For speed, this recommendation is based on a table of the shortest projected baselines for snapshots on the meridian in each of the four standard configurations, at 10° intervals in Declination.

`VLAUVPL` is an ancillary stand-alone program (or Lotus *1-2-3*-compatible spreadsheet) that can be used to refine the configuration recommendation. It computes the shortest projected VLA baseline for *full synthesis* observations between specified hour-angles at *any* Declination. It also generates u-v plots and graphs of $\sqrt{u^2 + v^2}$ versus hour-angle over the full range of hour-angles consistent with your prescribed elevation limits. These plits will help you to plan short-baseline coverage in detail. `VLAUVPL` is available by anonymous-ftp from `ftp.aoc.nrao.edu`, in the `pub/vlaplan` directory.

10.13 OBSERVE

When designing an observing strategy in detail, you may want to know more than just which calibration sources are near your targets. You may for example wish to estimate the calibration time overhead by calculating drive times, or to know if observations in the compact arrays will be affected by shadowing, etc. The *VLA Calibrator List* and a full model of the VLA on-line system (able to compute drive times and shadowing, etc.) are both included in the `OBSERVE` program. This program is designed to generate the text file that you would give the VLA operators in order to run the observations themselves, but it may also be useful if you want to pre-plan an observing run in detail. `OBSERVE` runs on Sun and IBM RS6000 workstations. It can be obtained from the NRAO by two routes:

1. by anonymous-ftp from directory `pub/observe` on `ftp.aoc.nrao.edu` (the preferred route), or

2. by regular mail on request from Theresa McBride in Socorro (`tmcbride@nrao.edu`, 505-835-7245); be prepared to specify the machine type (SUN, IBM) and a medium (diskette, Exabyte, DAT, etc.) on which you want receive the program.

Most users find that it takes a few hours to become conversant with `OBSERVE`. So, leave time to familiarize yourself with the program before you first use it! It is not something to be learned in a hurry just before a key deadline..... Help with `OBSERVE` is available from the AOC Data Analysts—Kevin Healy (505-835-7239) and Meri Stanley (505-835-7238)—or by E-mail from `analysts@nrao.edu`.

11 Acknowledgments

I thank Ron Ekers, Rick Perley, Fred Schwab, Jacqueline van Gorkom, Arnold Rots, and many students who attended earlier NRAO Summer Schools in Socorro, for valuable comments on previous versions of this lecture.

12 References

Adams, D. (1979), *The Hitch-Hiker's Guide to the Galaxy*, Pan Books, London.
Bridle, A. H. (1994), "VLAPLAN—VLA observing strategy planner", VLA Computer Memorandum No. 187, NRAO.
Bridle, A. H. and Schwab, F. R. (1989), "Wide-Field Imaging I: Bandwidth and Time-Average Smearing", Lecture 13 in *Synthesis Imaging in Radio Astronomy*, A.S.P. Conference Series, **6**, 247–256.
Clark, B. G. (1981), "Orders of magnitude of some instrumental effects", VLA Scientific Memorandum No. 137, NRAO.
Ledden, J. E., Broderick, J. J., Condon, J. J., and Brown, R. L. (1980), "A confusion-limited extragalactic source survey at 4.755 GHz. I. Source list and areal distributions", *Astron. J.*, **85**, 780–788.
Napier, P. J. and Rots, A. H. (1982), "VLA primary beam parameters", VLA Test Memorandum No. 134, NRAO.
Perley, R. A. (1988), "Calibration of P Band data", VLA Scientific Memorandum No. 159, NRAO.
Thompson, A. R. (1982), "The response of a radio-astronomy synthesis array to interfering signals", *IEEE Trans. Antennas Propagat.*, **AP-30**, 450–456.

Index